CR-61692
HREC-1095-1
LMSC/HREC A791267

LOCKHEED MISSILES & SPACE COMPANY
HUNTSVILLE RESEARCH & ENGINEERING CENTER
HUNTSVILLE RESEARCH PARK
4800 BRADFORD BLVD., HUNTSVILLE, ALABAMA

VIBRATIONAL CHARACTERISTICS OF ORTHOTROPIC SHELLS OF REVOLUTION

SUMMARY REPORT

March 1968

Contract NAS8-21095

by
K. R. Leimbach
C. E. Jones
W. D. Whetstone

APPROVED BY: Donald McDonald
D. McDonald, Manager
Structures & Mechanics

J. S. Farrior
J. S. Farrior
Resident Manager

FOREWORD

The work described in this report was performed by Lockheed Missiles & Space Company, Huntsville Research & Engineering Center, for the George C. Marshall Space Flight Center of the National Aeronautics and Space Administration under Contract NAS8-21095.

The work was administered under the direction of the Aero-Astrodynamics Laboratory, NASA/MSFC, with Dr. George F. McDonough as Contracting Officer Representative.

SUMMARY

This report describes a method of analysis and digital program for computing the vibrational mode shapes and frequencies of linear orthotropic shells of revolution. An approximate energy method (finite element) is employed, and solutions are computed using an iterative process similar to the Stodola-Vianello method for beam analysis.

In developing the program, primary emphasis was placed on numerical accuracy, generality, minimum input requirements, and economy of computer execution costs. One of the program's components which is independently useful for other applications is a very general routine for computing solutions corresponding to arbitrary static loadings.

Several examples are presented of solutions computed by the program.

CONTENTS

Section 1
INTRODUCTION

Exact analytical solutions to shell problems can be obtained in only a few special cases. Accordingly, in recent years attention has been directed toward developing computer-oriented methods of obtaining accurate approximate solutions to various general classes of shell problems.

Straightforward finite-difference equations have been used successfully in some applications. However, complicated problems (such as those involving irregular geometry) frequently involve solution of large numbers of poorly-conditioned simultaneous algebraic equations or high-order eigenproblems; accordingly, accumulation of arithmetic round-off error may be a significant factor.

The recent trend has been toward the use of finite element methods. The point of view usually taken in this approach is that the shell (or other structure) is represented as an assemblage of interconnected elements; and that the displacement field over the interior of each element is approximated as a specific function of the motion components of its boundary nodes. Alternatively, finite element techniques as usually applied may be regarded as approximate energy methods; and, provided that deformation compatibility requirements across all element boundaries are properly accounted for, the number and form of the displacement functions is entirely arbitrary. Without resorting to lumping of distributed mass or distributed applied forces at element boundaries, Lagrange's equation may be used to obtain system equations corresponding to the selected set of displacement functions. For free vibration of shells of revolution, independent sets of solutions exist for each circumferential wave number.

There are significant differences between ordinary finite-difference techniques and finite element methods which may be illustrated by the following example. Suppose a shell of revolution is analyzed in two different ways as follows:

1. The shell is represented as n annular finite elements of equal length. Within each element, the displacement field is approximated by a linear combination of eight independent functions, such that there is a one-to-one correspondence between the function coefficients, α_i (i=1 through 8), and the displacements and rotations of the element boundaries (i.e., the eight α's may be expressed in terms of the three displacements and the meridional rotation at the element's boundaries). Accordingly, all deformation compatibility requirements are identically satisfied if the 4(n+1) boundary motion components are chosen as generalized coordinates. (Some other 4(n+1) linear combinations of the 8n α's could have been selected as generalized coordinates, provided the compatibility requirements were properly accounted for.)

2. The problem is analyzed using a standard finite difference technique involving solution of four coupled difference equations in the three displacements and the meridional rotation. The difference net is composed of n+1 equally spaced points.

Similarities between the two approaches are evident; both involve a banded set of 4(n+1) algebraic equations in the same variables, namely the displacements and meridional rotations at n+1 equally spaced locations along the meridian of the shell. Accordingly, the computational efforts required to execute the two procedures would not differ substantially. However, it is generally the case* that unless n is very large, the energy method is substantially more accurate than the finite difference method. Also, accumulation of arithmetic round-off error increases substantially with large n, so that consideration of both computer execution cost and numerical accuracy strongly favors the energy method.

Investigators using finite difference methods have employed several different procedures to compute the free vibration characteristics of shells of revolution, including**:

---

*This is readily shown by comparison with exact solutions for a wide variety of static and dynamic beam, plate and shell problems.

**See e.g., Cohen (1964, 1965), Kalnins (1964, 1965), Klein (1964), and McDonald (1965).

1. Iteration of "assumed" frequencies until the required boundary conditions are closely approximated (similar to the well-known Myklestad method for computing beam modes and frequencies),
2. Iterative improvement of a succession of approximate mode shapes (similar to the Stodola-Vianello method applied to beams), using orthogonality relations to "sweep out" lower modes, in computing higher modes, and
3. Direct solution of large-order matrix eigenproblems of the form $(\omega^2 M - K) X = 0$, where the elements of the generalized coordinate vector X are the finite-difference variables.

Investigators using finite element methods have usually taken an approach similar to the last one outlined above, except that the generalized coordinates are the node point motion components. Using standard solution techniques (e.g., Cholesky-Givens, Wilkinson, etc.), this procedure is limited by steeply rising computer execution costs, numerical accuracy problems, and data storage limitations to relatively low order eigenproblems; accordingly, it is restricted to systems which can be well represented by a relatively small number of elements.

The formulation presented in this report uses a finite element approach. The solution technique used is an adaptation of the one described by Whetstone and Jones (1968) for computing the modes and frequencies of arbitrary linear space frames. In solving for the J^{th} mode (associated with a particular circumferential wave number), the state of the shell is characterized by the coefficients of J whole-structure displacement functions, the first J-1 of which are previously determined accurate approximations of the first J-1 modes, and the J^{th} function is an approximation of the J^{th} mode shape. The highest-frequency solution to the corresponding J^{th} order $(\omega^2 M - K)X = 0$ eigenproblem gives an interim approximation of the J^{th} mode, which in turn is used to compute an equivalent static loading from which a further improved approximation of the J^{th} mode is evaluated. This process is executed repeatedly until the desired accuracy is achieved.

Section 2
FREE VIBRATIONS

2.1 EQUATIONS OF MOTION

The free-vibration mode shapes of linear shells of revolution can easily be shown to be of the form

$$u(\xi,\varphi) = u^m(\xi)\cos m\varphi$$
$$v(\xi,\varphi) = v^m(\xi)\sin m\varphi$$
$$w(\xi,\varphi) = w^m(\xi)\cos m\varphi$$

where φ is the circumferential angle, ξ a meridional position coordinate, and u, v, and w the meridional, circumferential, and radial components, respectively, of the mode shapes. Except for a few special cases, the modal functions u^m, v^m, and w^m cannot be determined in closed form.

In the present analysis, shells of revolution are modeled as assemblages of finite elements, as shown on Figure 2-1. The elements are labled r = 1, (1), n and the element boundaries r = 1, (1), n+1.

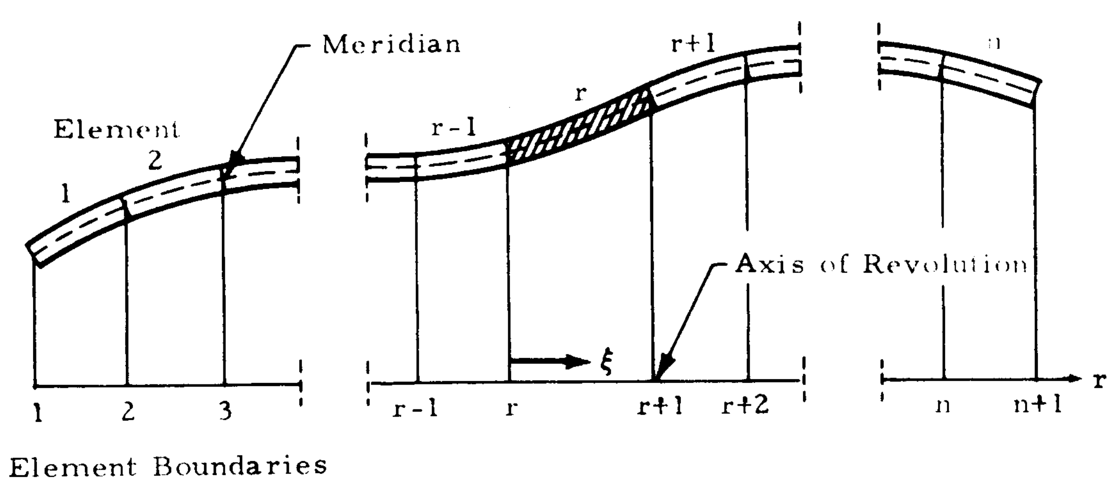

Figure 2-1 - Axial Section of Shell Model

In the finite element formulation, developed in detail in Sections 3 and 4, the displacement components over the interior of each element are approximated as cubic functions of the meridional position coordinate, ξ.

In terms of a set of generalized coordinates which will subsequently be discussed in detail, the kinetic and potential energies, T and V, respectively, of a shell may be written as follows:

$$T = \frac{1}{2} \sum_{i=1}^{N} \sum_{j=1}^{N} \dot{c}_i M_{ij} \dot{c}_j, \text{ and} \qquad (2\text{-}1)$$

$$V = \frac{1}{2} \sum_{i=1}^{N} \sum_{j=1}^{N} c_i K_{ij} c_j . \qquad (2\text{-}2)$$

The c_j's are coefficients of whole-shell displacement functions*, M_{ij} and K_{ij} are the generalized mass and stiffness coefficients, respectively, and $(\dot{\ }) = \frac{d}{dt}$.

The Lagrangian function is defined as

$$L = T - V , \qquad (2\text{-}3)$$

and Lagrange's equation for undamped free vibration is

$$\frac{d}{dt}\left(\frac{\partial L}{\partial \dot{c}_i}\right) - \frac{\partial L}{\partial c_i} = 0 \qquad i = 1, (1), N . \qquad (2\text{-}4)$$

Substitution of Equations (2-1) and (2-2) into (2-4) gives the equations

*The index, m, is omitted for convenience.

of motion as

$$\sum_{j=1}^{N} M_{ij}\,\ddot{c}_j + \sum_{j=1}^{N} K_{ij}\,c_j = 0 \qquad i = 1,(1),N\,. \tag{2-5}$$

Assuming solutions of Equation (2-5) of the form

$$c_j = \bar{c}_j \sin\omega t\,, \tag{2-6}$$

one obtains

$$\sum_{j=1}^{N} \omega^2 M_{ij}\,\bar{c}_j - \sum_{j=1}^{N} K_{ij}\,\bar{c}_j = 0 \qquad i = 1,(1),N\,. \tag{2-7}$$

Equation (2-7) is written in matrix form as

$$\omega^2 M\bar{c} - K\bar{c} = 0\,, \tag{2-8}$$

where M is the matrix of M_{ij}'s and K is the matrix of K_{ij}'s, termed the "mass" and "stiffness" matrices, respectively, and

$$\bar{c} = \begin{Bmatrix} \bar{c}_1 \\ \bar{c}_2 \\ \bar{c}_3 \\ \cdot \\ \cdot \\ \cdot \\ \bar{c}_N \end{Bmatrix}\,. \tag{2-9}$$

The M- and K-matrices must be determined for the whole shell, but, since the system is modeled as an assembly of finite elements, the kinetic and potential energies of a typical element are considered first.

In this formulation the generalized coordinates, c_j, j = 1, (1), N, are defined to be coefficients of displacement functions. Where $\bar{u}_j^r(\xi,\varphi)$, j = 1, (1), N, are the values of those functions over the r-th element, the deformation pattern of the r-th element for the m-th circumferential mode may be written as

$$u^r(\xi,\varphi,t) = \sum_{j=1}^{N} c_j \, \bar{u}_j^r(\xi,\varphi) \quad . \tag{2-10}$$

where

$$\bar{u}_j^r(\xi,\varphi) = \begin{Bmatrix} u_j^{mr}(\xi)\cos m\varphi \\ v_j^{mr}(\xi)\sin m\varphi \\ w_j^{mr}(\xi)\cos m\varphi \end{Bmatrix} . \tag{2-11}$$

For simplicity in formulating the potential energy, it is assumed that the static loading function is known which produces the deformation pattern $\bar{u}_j^r(\xi,\varphi)$. It is expressed as

$$\bar{p}_j^r(\xi,\varphi) = \begin{Bmatrix} p_{uj}^{mr}(\xi)\cos m\varphi \\ p_{vj}^{mr}(\xi)\sin m\varphi \\ p_{wj}^{mr}(\xi)\cos m\varphi \end{Bmatrix} , \tag{2-12}$$

so that

$$p^r(\xi,\varphi,t) = \sum_{j=1}^{N} c_j \, \bar{p}_j^r(\xi,\varphi) . \tag{2-13}$$

The components u_j^{mr}, v_j^{mr}, and w_j^{mr}, and the coordinates ξ and φ are defined in Section A.1. The load components p_{uj}^{mr}, p_{vj}^{mr}, and p_{wj}^{mr} correspond in direction to u, v, and w, respectively.

The mass per unit area is given by

$$\mu(\xi) = \rho\, h(\xi) \tag{2-14}$$

where ρ is the mass per unit volume, and $h(\xi)$ is the shell thickness. With the metric coefficients $A(\xi)$ and $R(\xi)$, defined in Section A.1, and with the effect of rotatory inertia neglected, the kinetic energy of the r-th element is

$$T^r = \frac{1}{2}\int_0^{2\pi}\int_0^{L_r} \mu(\xi) \sum_{i=1}^{N} \dot{c}_i\, \overline{u}_i^{r*}(\xi,\varphi) \sum_{j=1}^{N} \dot{c}_j\, \overline{u}_j^{r}(\xi,\varphi)\, A(\xi)\, R(\xi)\, d\xi\, d\varphi =$$

$$= \frac{1}{2}\sum_{i=1}^{N}\sum_{j=1}^{N} \dot{c}_i \left[\int_0^{2\pi}\int_0^{L_r} \mu(\xi)\, \overline{u}_i^{r*}(\xi,\varphi)\, \overline{u}_j^{r}(\xi,\varphi)\, A(\xi)\, R(\xi)\, d\xi\, d\varphi\right] \dot{c}_j\,, \tag{2-15}$$

where L_r is the length of the element r.

Similarly, the potential energy of the r-th element is

$$V^r = \frac{1}{2}\int_0^{2\pi}\int_0^{L_r} \sum_{i=1}^{N} c_i\, \overline{u}_i^{r*}(\xi,\varphi) \sum_{j=1}^{N} c_j\, \overline{p}_j^{r}(\xi,\varphi)\, A(\xi)\, R(\xi)\, d\xi\, d\varphi =$$

$$= \frac{1}{2}\sum_{i=1}^{N}\sum_{j=1}^{N} c_i \left[\int_0^{2\pi}\int_0^{L_r} \overline{u}_i^{r*}(\xi,\varphi)\, \overline{p}_j^{r}(\xi,\varphi)\, A(\xi)\, R(\xi)\, d\xi\, d\varphi\right] c_j\,. \tag{2-16}$$

The two integrals are defined as

$$\overline{M}_{ij}^{r} = \int_0^{2\pi}\int_0^{L_r} \mu(\xi)\, \overline{u}_i^{r*}(\xi,\varphi)\, \overline{u}_j^{r}(\xi,\varphi)\, A(\xi)\, R(\xi)\, d\xi\, d\varphi\,, \tag{2-17}$$

and

$$\overline{K}_{ij}^{r} = \int_0^{2\pi}\int_0^{L_r} \overline{u}_i^{r*}(\xi,\varphi)\, \overline{p}_j^{r}(\xi,\varphi)\, A(\xi)\, R(\xi)\, d\xi\, d\varphi\,, \tag{2-18}$$

so that

$$T^r = \frac{1}{2} \sum_{i=1}^{N} \sum_{j=1}^{N} \dot{c}_i \, \overline{M}^r_{ij} \, \dot{c}_j \text{ , and} \tag{2-19}$$

$$V^r = \frac{1}{2} \sum_{i=1}^{N} \sum_{j=1}^{N} c_i \, \overline{K}^r_{ij} \, c_j \text{ .} \tag{2-20}$$

The kinetic and potential energies of the whole shell are

$$T = \sum_{r=1}^{n} T^r = \frac{1}{2} \sum_{i=1}^{N} \sum_{j=1}^{N} \dot{c}_i \left[\sum_{r=1}^{n} \overline{M}^r_{ij} \right] \dot{c}_j \text{ , and} \tag{2-21}$$

$$V = \sum_{r=1}^{n} V^r = \frac{1}{2} \sum_{i=1}^{N} \sum_{j=1}^{N} c_i \left[\sum_{r=1}^{n} \overline{K}^r_{ij} \right] c_j \text{ .} \tag{2-22}$$

Comparison with Equations (2-1) and (2-2) shows that

$$M_{ij} = \sum_{r=1}^{n} \overline{M}^r_{ij} \text{ , and} \tag{2-23}$$

$$K_{ij} = \sum_{r=1}^{n} \overline{K}^r_{ij} \text{ .} \tag{2-24}$$

2.2 SOLUTION BY ITERATION

Solutions to Equation (2-8) can be accurately obtained by means of several well known numerical methods, provided the equations are well conditioned and not of too high order. These conditions are obviously dependent upon the number and nature of the generalized coordinates.

The following discussion is concerned with whole-shell deformation patterns corresponding to particular static loadings as coordinates.

Suppose the shell is subjected to a set of static loading functions of the form of Equation (2-12), and the corresponding deformation pattern is determined. If N functions are used, an N-th order eigenproblem of the form of Equation (2-8) arises, in which the coordinates, c_j, are simply coefficients of the N whole shell deformation patterns.

The success of this method is contingent upon a judicious choice of loading functions. An iterative procedure for obtaining a succession of improved functions is discussed below and the method used for static analysis is presented in Section 3.

Suppose that very accurate approximations to the first N-1 modes are known. Then, if one chooses those functions as the first N-1 displacement functions corresponding to generalized coordinates c_1, c_2, ..., c_{N-1}, and, in addition, a function approximating the N-th mode, the matrices in Equation (2-8) appear as

$$\overset{(1)}{M} = \begin{bmatrix} M_{11} & M_{12} & M_{13} & \cdot & \cdot & \cdot & \overset{(1)}{M}_{1N} \\ & M_{22} & M_{23} & \cdot & \cdot & \cdot & \overset{(1)}{M}_{2N} \\ & & M_{33} & \cdot & \cdot & \cdot & \overset{(1)}{M}_{3N} \\ & & & \cdot & & & \cdot \\ & & & & \cdot & & \cdot \\ & & & & & \cdot & \cdot \\ \text{Symmetric} & & & & & & \overset{(1)}{M}_{NN} \end{bmatrix}, \text{ and}$$

$$\overset{(1)}{K} = \begin{bmatrix} K_{11} & K_{12} & K_{13} & \cdot & \cdot & \cdot & \overset{(1)}{K}_{1N} \\ & K_{22} & K_{23} & \cdot & \cdot & \cdot & \overset{(1)}{K}_{2N} \\ & & K_{33} & \cdot & \cdot & \cdot & \overset{(1)}{K}_{3N} \\ & & & \cdot & & & \cdot \\ & & & & \cdot & & \cdot \\ & & & & & \cdot & \cdot \\ \text{Symmetric} & & & & & & \overset{(1)}{K}_{NN} \end{bmatrix} \tag{2-25}$$

The superscript (1) denotes the first approximation to the N-th mode shape. Solutions to Equation (2-8) are the previously determined first N-1 modes, and an upper bound approximation to the N-th system mode. Therefore, the first N-1 eigenvectors are nearly* of the form

$$\begin{Bmatrix} 1 \\ 0 \\ 0 \\ \cdot \\ \cdot \\ \cdot \\ 0 \\ 0 \end{Bmatrix}, \begin{Bmatrix} 0 \\ 1 \\ 0 \\ \cdot \\ \cdot \\ \cdot \\ 0 \\ 0 \end{Bmatrix}, \begin{Bmatrix} 0 \\ 0 \\ 1 \\ \cdot \\ \cdot \\ \cdot \\ 0 \\ 0 \end{Bmatrix}, \begin{Bmatrix} 0 \\ 0 \\ 0 \\ \cdot \\ \cdot \\ \cdot \\ 1 \\ 0 \end{Bmatrix}, \text{ respectively.}$$

*If the first N-1 modes were known exactly, the eigenvectors would be as shown; however, some residual arithmetic error is always present, so that these functions are not identically orthogonal. Instead, the terms shown as zeros are actually numbers of magnitude much smaller than unity.

The eigenvector, $\overset{(1)}{\bar{c}}_N$, associated with the highest frequency solution, $\overset{(1)}{\omega}_N$, of Equation (2-8) is represented as

$$\overset{(1)}{c}_N = \begin{Bmatrix} \overset{(1)}{\bar{c}}_{1N} \\ \overset{(1)}{\bar{c}}_{2N} \\ \overset{(1)}{\bar{c}}_{3N} \\ \cdot \\ \cdot \\ \cdot \\ \overset{(1)}{\bar{c}}_{NN} \end{Bmatrix} \tag{2-26}$$

From Equation (2-10) one obtains the first interim approximation to the N-th system mode as a set of elemental deformation patterns defined as

$$\overset{(1)}{\tilde{u}}{}^r_N (\xi, \varphi) = \sum_{j=1}^{N} \overset{(1)}{c}_{jN} \, \bar{u}^r_j (\xi, \varphi) \tag{2-27}$$

where $\bar{u}^r_j (\xi, \varphi)$, as defined by Equation (2-11), describes the deformation of the r-th element associated with the j-th whole-shell mode shape.

After such an approximate solution has been computed an improved approximation can be calculated as follows. From the interim approximations a set of element inertial loading functions is generated as

$$\overset{(2)}{\bar{p}}{}^r_N (\xi, \varphi) = \rho \, h(\xi) \, \overset{(1)}{\tilde{u}}{}^r_N (\xi, \varphi) \tag{2-28}$$

The deformation of the shell corresponding to this static loading is the second approximation to the N-th system mode. The procedure is repeated until satisfactory convergence is reached.

Several criteria are available for determining acceptable convergence; some of these are

(a) $\omega_N^{(\ell)}$ is approximately equal to $\omega_N^{(\ell-1)}$

(b) $M_{iN}^{(\ell)}$ and $K_{iN}^{(\ell)}$ are much smaller than $M_{NN}^{(\ell)}$ and $K_{NN}^{(\ell)}$, respectively, for i = 1, (1), N-1.

(c) $\overline{c}_{iN}^{(\ell)}$ are much smaller than $\overline{c}_{NN}^{(\ell)}$ for i = 1, (1), N-1.

It is interesting to note that the off-diagonal terms of Equation (2-25) except those of the N-th rows and columns are many orders of magnitude smaller than the diagonal terms. This is a result of orthogonality of the free vibration modes 1 through N-1.

Initial approximations may be prescribed either by directly stating the displacement field or by allowing the program to compute the displacement function corresponding to a specified static loading. Experience has revealed that crude approximations are adequate because of the rapidity of convergence of the repetitive solution technique.

The only obvious pitfall in selecting an initial approximation is that of choosing a deformation pattern for the N-th system mode which is a linear combination of modes 1 through N-1. In this case the matrices of Equations (2-25) are singular. This error is more likely to occur with higher values of N; therefore, since lower system modes are usually of primary concern and the probability of such an occurrence is slight, this is not considered a serious weakness of the method.

Section 3
STATIC ANALYSIS

Execution of the repetitive procedure described in the preceding section requires solutions to statically loaded finite element shell assemblies with specified boundary conditions, that is, displacement fields, $\mathscr{D}$, have to be obtained for given static loading functions, $\mathscr{P}$.

These solutions are obtained through application of the theorem of superposition for linear structures so that the desired complete displacement fields are given by

$$\mathscr{D} = \mathscr{D}_1 + \mathscr{D}_2 .$$

$\mathscr{D}_1$ is the displacement field obtained by restraining all element boundary motions and subjecting the "fixed edge" elements to the loading, $\mathscr{P}$. With element boundaries unrestrained (except for specified boundary conditions), $\mathscr{D}_2$ is the displacement field produced by $-\mathscr{F}$, where $\mathscr{F}$ is the set of element boundary reaction loads corresponding to $\mathscr{D}_1$.

A variation of this method is described below. It is a state vector "walk-through" procedure, in which, unless otherwise specified, primed quantities refer to the right boundary and unprimed quantities to the left boundary of an element.

The total forces, f^t and $f^{t'}$, at the boundaries of the r-th element may be represented as

$$\begin{Bmatrix} f^t(r) \\ f^{t'}(r) \end{Bmatrix} = \begin{Bmatrix} f(r) \\ f'(r) \end{Bmatrix} + \begin{Bmatrix} f^f(r) \\ f^{f'}(r) \end{Bmatrix} \quad (3\text{-}1)$$

where f , f' are the forces required at the boundaries of an unloaded element subjected to boundary deformation, and f^f , $f^{f'}$ are the forces required at the boundaries of an element subjected to applied surface loading and restrained against boundary deformation. The latter are termed fixed edge forces.

The boundary force-displacement relationship of the r-th finite element is expressed as

$$\begin{Bmatrix} f(r) \\ \hline f'(r) \end{Bmatrix} = \left[\begin{array}{c:c} K_{11}(r) & K_{12}(r) \\ \hdashline K_{21}(r) & K_{22}(r) \end{array}\right] \begin{Bmatrix} q(r) \\ \hline q'(r) \end{Bmatrix} \tag{3-2}$$

so that the total forces are

$$\begin{Bmatrix} f^t(r) \\ \hline f^{t'}(r) \end{Bmatrix} = \left[\begin{array}{c:c} K_{11}(r) & K_{12}(r) \\ \hdashline K_{21}(r) & K_{22}(r) \end{array}\right] \begin{Bmatrix} q(r) \\ \hline q'(r) \end{Bmatrix} + \begin{Bmatrix} f^f(r) \\ \hline f^{f'}(r) \end{Bmatrix} \tag{3-3}$$

where $q(r)$ and $q'(r)$ represent the three displacement components and the meridional rotation of the left and right boundary, respectively, and

$$\begin{bmatrix} K_{11}(r) & K_{12}(r) \\ K_{21}(r) & K_{22}(r) \end{bmatrix}$$

is the r-th element stiffness matrix. The derivation of this relation is presented in Section 4.

Equation (3-3) is rearranged to give an explicit expression for q' and $f^{t'}$, so that

$$\begin{Bmatrix} q'(r) \\ f^{t'}(r) \end{Bmatrix} = \left[\begin{array}{c:c} -K_{12}^{-1}\ K_{11} & K_{12}^{-1} \\ \hdashline K_{21} - K_{22}\ K_{12}^{-1}\ K_{11} & K_{22}\ K_{12}^{-1} \end{array}\right]_{(r)} \begin{Bmatrix} q(r) \\ f^{t}(r) \end{Bmatrix} +$$

$$+ \left[\begin{array}{c:c} -K_{12}^{-1} & \Phi_4 \\ \hdashline -K_{22}\ K_{12}^{-1} & I_4 \end{array}\right]_{(r)} \begin{Bmatrix} f^{f}(r) \\ f^{f'}(r) \end{Bmatrix} . \quad (3\text{-}4)^*$$

To simplify Equation (3-4), the vectors,

$$\begin{Bmatrix} q'(r) \\ f^{t'}(r) \end{Bmatrix} \quad \text{and} \quad \begin{Bmatrix} q(r) \\ f^{t}(r) \end{Bmatrix}$$

are defined as state vectors, s′ and s, respectively, and the matrix

$$\overline{T}(r) = \left[\begin{array}{c:c} -K_{12}^{-1}\ K_{11} & K_{12}^{-1} \\ \hdashline K_{21} - K_{22}\ K_{12}^{-1}\ K_{11} & K_{22}\ K_{12}^{-1} \end{array}\right]_{(r)} , \qquad (3\text{-}5)$$

and the vector

$$\overline{g}(r) = \left[\begin{array}{c:c} K_{12}^{-1} & \Phi_4 \\ \hdashline -K_{22}\ K_{12}^{-1} & I_4 \end{array}\right]_{(r)} \begin{Bmatrix} f^{f}(r) \\ f^{f'}(r) \end{Bmatrix} \qquad (3\text{-}6)$$

are termed the transfer matrix and the load vector, respectively. Equation (3-4) can now be written as

---

*Φ_4 and I_4 represent 4-th order zero and identity matrices, respectively.

$$s'(r) = \overline{T}(r)\, s(r) + \overline{g}(r) \tag{3-7}$$

for the r-th element.

Compatibility of deformations and equilibrium of forces are required at the (r+1)-th element boundary common to the two contiguous elements (r) and (r+1). Deformation compatibility is given by

$$q'(r) = q(r+1)\ . \tag{3-8}$$

Force equilibrium is described by the following equation

$$f^{t'}(r) + f^{t}(r+1) + \overline{K}(r+1)\, q'(r) + \overline{p}(r+1) = 0\ , \tag{3-9}$$

where $\overline{K}(r+1)$ reflects an attached elastic ring system at the element boundary (r+1), and $\overline{p}(r+1)$ is an externally applied ring load.

Equations (3-8) and (3-9) can be combined into a matrix equation of the form

$$s(r+1) = J(r+1)\, s'(r) + p(r+1) \tag{3-10}$$

where

$$J(r+1) = \left[\begin{array}{c|c} I_4 & \Phi_4 \\ \hline -K(r+1) & -I_4 \end{array}\right]\ , \quad \text{and}$$

$$p\,(r+1) = \left\{\begin{array}{c} 0 \\ \hline -\overline{p}(r+1) \end{array}\right\}\ .$$

Substituting Equation (3-7) into (3-10), one obtains the governing difference equation with variable coefficients as

$$s(r+1) = J(r+1)\,\overline{T}(r)\, s(r) + J(r+1)\,\overline{g}(r) + p(r+1)\ . \tag{3-11}$$

For the more common case of $\overline{K}(r+1) = 0$ and $\overline{p}(r+1) = 0$ Equation (3-11) simplifies to

$$s(r+1) = J\left(\overline{T}(r)\ s(r) + \overline{g}(r)\right)$$

in which

$$J = \left[\begin{array}{c|c} I_4 & 0 \\ \hline 0 & -I_4 \end{array}\right]$$

with

$$T(r) = J\,\overline{T}(r) \quad \text{and} \quad g(r) = J\,\overline{g}(r)$$

Equation (3-11) becomes

$$s(r+1) = T(r)\ s(r) + g(r)\ . \tag{3-12}$$

As outlined below the solution to this difference equation is obtained in two steps:

(a) the unknown quantities of the two states $s(1)$ and $s(n+1)$ are found for given boundary conditions and given loads,

(b) the interior states are computed from the difference equation (3-12) using $s(1)$ as an initial vector.

From Equation (3-12)

$$s(2) = T(1)\ s(1) + g(1)$$

$$s(3) = T(2)\ T(1)\ s(1) + T(2)\ g(1) + g(2)$$

$$\vdots$$

$$s(n+1) = \left(\prod_{r=1}^{n}{}^{*}\, T(r)\right)^{*} s(1) + \sum_{r=1}^{n-1}\left[\left(\prod_{j=r+1}^{n}{}^{*}\, T(j)\right)^{*} g(r)\right] + g(n) \equiv A\ s(1) + e\ . \qquad (3\text{-}13)^{*}$$

---

* $\prod_{i=1}^{n} x_i = x_1\, x_2\, x_3 \cdots x_n$

Equation (3-13) is simplified to

$$y = A\,x + e \tag{3-14}$$

where

$$y = s(n+1) \quad \text{and} \quad x = s(1)\,.$$

The boundary state vectors are partitioned into known and unknown quantities so that

$$\begin{Bmatrix} \bar{x}_k \\ \bar{x}_u \end{Bmatrix} = \bar{x} = P_x\,x\,, \quad \begin{Bmatrix} \bar{y}_k \\ \bar{y}_u \end{Bmatrix} = \bar{y} = P_y\,y \tag{3-15}$$

in which $\bar{x}_k$, $\bar{y}_k$ are the known, $\bar{x}_u$, $\bar{y}_u$ are the unknown quantities, and P_x, P_y are permutation matrices*. Equation (3-14) can now be rewritten as

$$\bar{y} = P_y\,A\,P_x^{-1}\,\bar{x} + P_y\,e\,. \tag{3-16}$$

With

$$\bar{A} = P_y\,A\,P_x^{-1}\,, \quad \text{and}$$

$$\bar{e} = P_y\,e$$

Equation (3-16) becomes

$$\bar{y} = \bar{A}\,\bar{x} + \bar{e}\,. \tag{3-17}$$

The unknown boundary quantities are determined by partitioning Equation (3-17) in the following manner:

$$\begin{Bmatrix} \bar{y}_k \\ \hline \bar{y}_u \end{Bmatrix} = \left[\begin{array}{c:c} \bar{A}_{11} & \bar{A}_{12} \\ \hdashline \bar{A}_{21} & \bar{A}_{22} \end{array}\right] \begin{Bmatrix} \bar{x}_k \\ \hline \bar{x}_u \end{Bmatrix} + \begin{Bmatrix} \bar{e}_1 \\ \hline \bar{e}_2 \end{Bmatrix}$$

---

*Permutation matrices for various boundary conditions are discussed in Appendix A.3.

and solving for $\bar{x}_u$ and $\bar{y}_u$, so that

$$\begin{Bmatrix} \bar{x}_u \\ \hline \bar{y}_u \end{Bmatrix} = \left[\begin{array}{c|c} -\bar{A}_{12}^{-1} \; \bar{A}_{11} & \bar{A}_{12}^{-1} \\ \hline \bar{A}_{21} \; -\bar{A}_{22} \; \bar{A}_{12}^{-1} \; \bar{A}_{11} & \bar{A}_{22} \; \bar{A}_{12}^{-1} \end{array}\right] \begin{Bmatrix} \bar{x}_k \\ \bar{y}_k \end{Bmatrix} + \left[\begin{array}{c|c} -\bar{A}_{12}^{-1} & 0 \\ \hline -\bar{A}_{22} \; \bar{A}_{12}^{-1} & I_4 \end{array}\right] \begin{Bmatrix} \bar{e}_1 \\ \bar{e}_2 \end{Bmatrix} \tag{3-19}$$

The solution may be written in two vector equations as

$$\bar{x}_u = \bar{A}_{12}^{-1} (\bar{y}_k - \bar{A}_{11} \bar{x}_k - \bar{e}_1) , \quad \text{and}$$

$$\bar{y}_u = \bar{A}_{21} \bar{x}_k + \bar{A}_{22} \bar{x}_u + \bar{e}_2 . \tag{3-20}$$

For cases in which the known boundary quantities are zero, the solution is

$$\bar{x}_u = -\bar{A}_{12}^{-1} \bar{e}_1$$

$$\bar{y}_u = \bar{A}_{22} \bar{x}_u + \bar{e}_2 . \tag{3-21}$$

The state at $r=1$ is

$$x = P_x^{-1} \bar{x} = s(1) ,$$

and the states at $r=2, (1), n$ are obtained by successive use of Equation (3-12).

Section 4
FINITE ELEMENT

4.1 GENERAL

In recent years the literature on finite element methods and various types of elements has increased so vastly that only a few of the papers can be mentioned here.

To analyze a structural system composed of an assemblage of finite elements and exposed to an arbitrary loading, one must obtain for each element

1. Equations relating the boundary displacements to the boundary forces of the element not subjected to any distributed loading.
2. Boundary forces required to equilibrate the loaded element when its boundary displacements are identically equal to zero or, "fixed".

Relations between boundary displacements and forces were derived by Gallagher (1963) in matrix form. A stiffness matrix was derived with an assumed meridional power series displacement pattern in which the number of coefficients was equal to the number of generalized boundary displacements of the element. Pian (1964) showed by the principle of minimum potential energy that taking more terms in the displacement function improved equilibrium in the interior of the element and led to an improved stiffness matrix. Klein (1964) applied both methods to various structural elements (such as straight and curved beams, circular plates, and cylindrical and conical shells). Instead of computing the true fixed-edge forces, he simply lumped the external loading at the boundaries of the elements.

In the following two parts of this section the stiffness matrix and the fixed-edge forces are derived for an element of a shell of revolution.

The finite element is chosen to approximate any given shell of revolution as closely as possible. The fixed edge forces are found by the use of influence functions.

4.2 STIFFNESS MATRIX

In previous finite element analyses, shells of revolution were discussed as assemblies of conical frusta. This modeling introduced residual moments due to the abrupt change of meridional slope. It is therefore desirable to use a shell element that will match the meridional radii and slopes of the model at the element boundaries with those of the actual structure. Such an element is one with a curved meridian as shown on Figure 4-1.

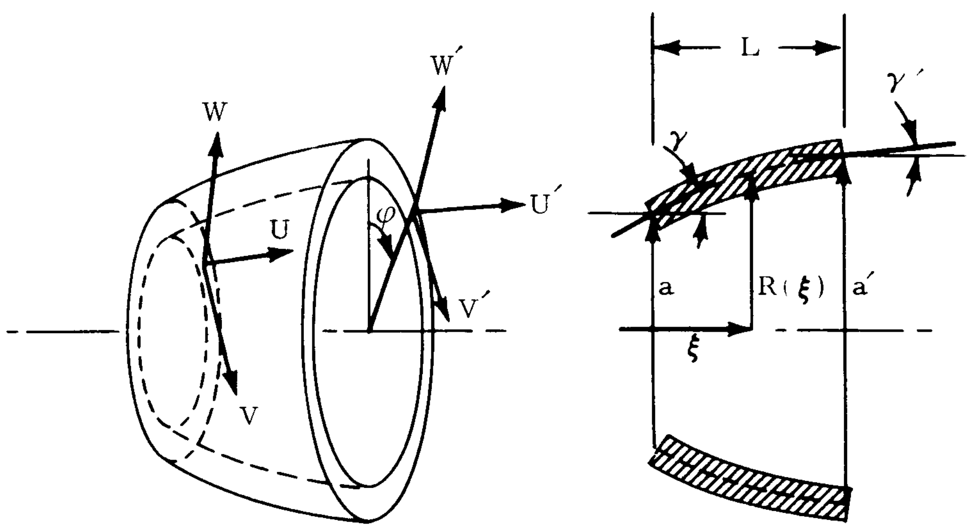

(a) Isometric View (b) Section Parallel to Axis

Figure 4-1 - Shell Element with Curved Meridian

For this element, the radius as a function of the coordinate ξ as shown on Figure 4-1b is assumed to be

$$R(\xi) = a_0 + a_1 \xi + a_2 \xi^2 + a_3 \xi^3$$

where

$$\begin{aligned}
a_0 &= a \\
a_1 &= \tan\gamma \\
a_2 &= -\frac{1}{L}(\tan\gamma' + 2\tan\gamma) - \frac{3}{L^2}(a - a') \\
a_3 &= -\frac{1}{L^2}(\tan\gamma' + \tan\gamma) + \frac{2}{L^2}(a - a')
\end{aligned} \tag{4-1}$$

Two special cases are the conical element, where

$$a_0 = a, \quad a_1 = \tan\gamma, \quad a_2 = a_3 = 0,$$

and the cylindrical element, where

$$a_0 = a, \quad a_1 = a_2 = a_3 = 0.$$

The displacement pattern of an element is characterized as a power series along its meridian and a Fourier expansion in its circumferential angle, so that

$$\begin{aligned}
u(\xi,\varphi) &= \sum_{m=0}^{\infty} u_m(\xi) \cos m\varphi, \\
v(\xi,\varphi) &= \sum_{m=0}^{\infty} v_m(\xi) \sin m\varphi, \quad \text{and} \\
w(\xi,\varphi) &= \sum_{m=0}^{\infty} w_m(\xi) \cos m\varphi
\end{aligned} \tag{4-2}$$

where

$$
\begin{aligned}
u_m(\xi,\varphi) &= \alpha_5^m + \alpha_6^m\xi + \alpha_9\xi^2 + \alpha_{10}^m\xi^3 \\
v_m(\xi,\varphi) &= \alpha_7^m + \alpha_8^m\xi + \alpha_{11}^m\xi^2 + \alpha_{12}^m\xi^3 \\
w_m(\xi,\varphi) &= \alpha_1^m + \alpha_2^m\xi + \alpha_3^m\xi^2 + \alpha_4^m\xi^3 \qquad (4\text{-}3)
\end{aligned}
$$

The coefficients α_i^m are labeled in this particular pattern to place emphasis on the w-displacement.

The rotation of the meridian can be derived from Figure 4-2.

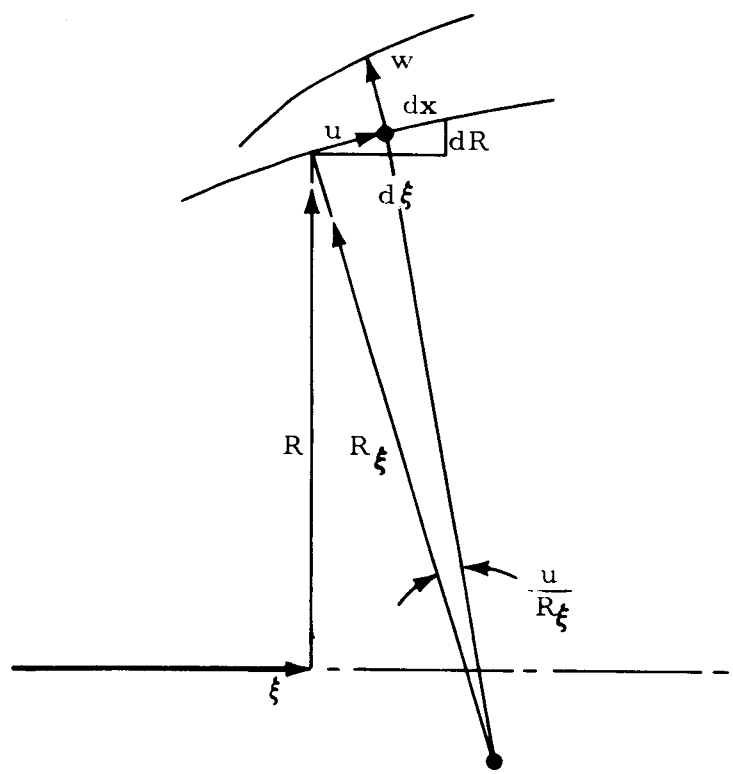

Figure 4-2 - Rotation of the Meridian

From Equation (A-5) in the Appendix

$$dx = A\, d\xi \ ,$$

so that the rotation of the meridian is expressed by

$$\theta_m(\xi) = \frac{1}{A} w_m'(\xi) - \frac{1}{R_\xi} u_m(\xi) \tag{4-4}$$

where $(\ )' = \frac{\partial}{\partial \xi}$.

The boundary displacements are represented by U, V, W, and U′, V′, W′ as shown on Figure 4-1a, and the meridional rotations of the boundaries are denoted by θ and θ'. The boundary stress resultants are shown on Figure 4-3, where S and T are the effective out-of-plane and in-plane shears, respectively. All boundary forces are assumed to be positive in the direction of positive boundary displacements.

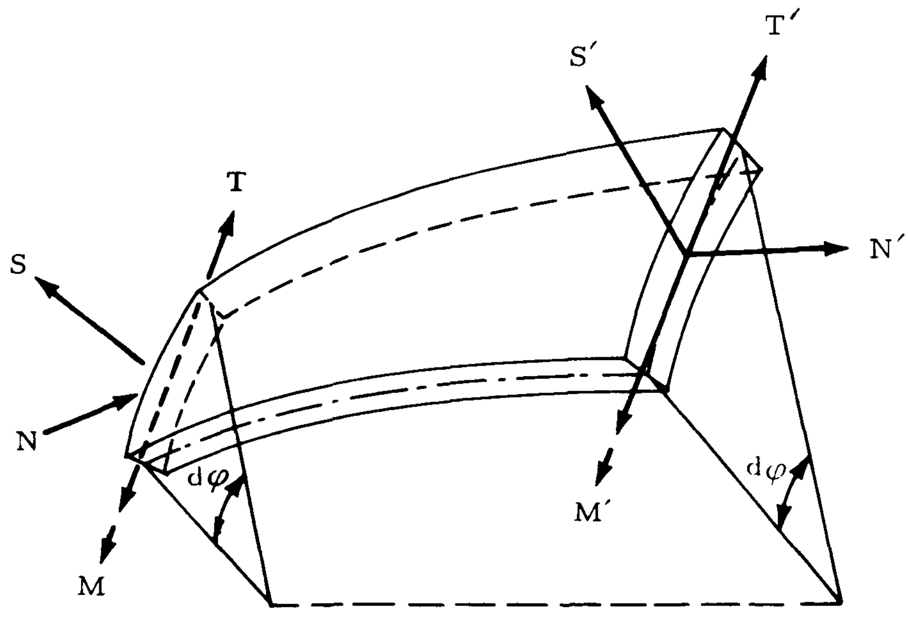

Figure 4-3 - Boundary Forces on Shell Element

Considering the m-th term of the Fourier expansion, called the m-th harmonic, one can define an elemental stiffness matrix, K_m, which relates the boundary forces to the boundary displacements, so that

$$f_m = K_m q_m \tag{4-5}$$

in which

$$f_m = \begin{Bmatrix} N_m \\ T_m \\ S_m \\ M_m \\ N'_m \\ T'_m \\ S'_m \\ M'_m \end{Bmatrix}, \quad \text{and} \quad q_m = \begin{Bmatrix} U_m \\ V_m \\ W_m \\ \theta_m \\ U'_m \\ V'_m \\ W'_m \\ \theta'_m \end{Bmatrix} \tag{4-6}$$

Evaluation of Equations (4-3) and (4-4) at the boundaries ξ=0 and ξ=L gives

$$\begin{Bmatrix} U_m \\ V_m \\ W_m \\ \theta_m \\ U'_m \\ V'_m \\ W'_m \\ \theta'_m \end{Bmatrix} = \underbrace{\left[\begin{array}{cccccccc|cccc} 0 & 0 & 0 & 0 & 1 & 0 & 0 & 0 & 0 & 0 & 0 & 0 \\ 0 & 0 & 0 & 0 & 0 & 0 & 1 & 0 & 0 & 0 & 0 & 0 \\ 1 & 0 & 0 & 0 & 0 & 0 & 0 & 0 & 0 & 0 & 0 & 0 \\ 0 & \frac{1}{\lambda_1} & 0 & 0 & \frac{1}{\lambda_3} & 0 & 0 & 0 & 0 & 0 & 0 & 0 \\ 0 & 0 & 0 & 0 & 1 & L & 0 & 0 & L^2 & L^3 & 0 & 0 \\ 0 & 0 & 0 & 0 & 0 & 0 & 1 & L & 0 & 0 & L^2 & L^3 \\ 1 & L & L^2 & L^3 & 0 & 0 & 0 & 0 & 0 & 0 & 0 & 0 \\ 0 & \frac{1}{\lambda_2} & \frac{2L}{\lambda_2} & \frac{3L^2}{\lambda_2} & \frac{1}{\lambda_4} & \frac{L}{\lambda_4} & 0 & 0 & \frac{L^2}{\lambda_4} & \frac{L^3}{\lambda_4} & 0 & 0 \end{array}\right]}_{8\times 8 \qquad\qquad 8\times 4} \begin{Bmatrix} \alpha_1^m \\ \alpha_2^m \\ \alpha_3^m \\ \alpha_4^m \\ \alpha_5^m \\ \alpha_6^m \\ \alpha_7^m \\ \alpha_8^m \\ \hline \alpha_9^m \\ \alpha_{10}^m \\ \alpha_{11}^m \\ \alpha_{12}^m \end{Bmatrix} \tag{4-7}$$

where

$$\lambda_1 = \sqrt{1 + a_1^2} ,$$

$$\lambda_2 = \sqrt{1 + \left(a_1 + 2a_2 L + 3a_3 L^2\right)^2} ,$$

$$\lambda_3 = \lambda_1^3 (2a_2)^{-1}, \quad \text{and}$$

$$\lambda_4 = \lambda_2^3 (2a_2 + 6a_3 L)^{-1} .$$

Equation (4-7) is written more compactly as

$$q_m = \left(\mathbb{B}_a \;\vdots\; \mathbb{B}_b \right) \begin{Bmatrix} \alpha_a^m \\ \hline \alpha_b^m \end{Bmatrix} . \tag{4-8}$$

A matrix, $\mathbb{M}$, is now defined by the following relation

$$\mathbb{M} = \left[\begin{array}{c|c} \mathbb{B}_a^{-1} & -\mathbb{B}_a^{-1} \mathbb{B}_b \\ \hline 0 & I_4 \end{array} \right]_{12 \times 12}$$

so that

$$\alpha^m = \begin{Bmatrix} \alpha_a^m \\ \hline \alpha_b^m \end{Bmatrix} = \mathbb{M} \begin{Bmatrix} q_m \\ \hline \alpha_b^m \end{Bmatrix} \tag{4-9}$$

The submatrices of $\mathbf{M}$ are as follows:

$$
\mathbf{B}_a^{-1} = \begin{bmatrix}
0 & 0 & 1 & 0 & 0 & 0 & 0 & 0 \\
-\bar{\lambda}_3 & 0 & 0 & \lambda_1 & 0 & 0 & 0 & 0 \\
\frac{2\bar{\lambda}_3}{L} & 0 & -\frac{3}{L^2} & -\frac{2\lambda_1}{L} & \frac{\bar{\lambda}_4}{L} & 0 & \frac{3}{L^2} & -\frac{\lambda_2}{L} \\
-\frac{\bar{\lambda}_3}{L^2} & 0 & \frac{2}{L^3} & \frac{\lambda_1}{L^2} & -\frac{\bar{\lambda}_4}{L^2} & 0 & -\frac{2}{L^3} & \frac{\lambda_2}{L^2} \\
1 & 0 & 0 & 0 & 0 & 0 & 0 & 0 \\
-\frac{1}{L} & 0 & 0 & 0 & \frac{1}{L} & 0 & 0 & 0 \\
0 & 1 & 0 & 0 & 0 & 0 & 0 & 0 \\
0 & -\frac{1}{L} & 0 & 0 & 0 & \frac{1}{L} & 0 & 0
\end{bmatrix}
$$

in which $\bar{\lambda}_3 = \frac{\lambda_1}{\lambda_3}$ and $\bar{\lambda}_4 = \frac{\lambda_2}{\lambda_4}$,

$$-\mathbf{B}_a^{-1}\ \mathbf{B}_b = \begin{bmatrix} 0 & 0 & 0 & 0 \\ 0 & 0 & 0 & 0 \\ 0 & 0 & 0 & 0 \\ 0 & 0 & 0 & 0 \\ 0 & 0 & 0 & 0 \\ -L & -L^2 & 0 & 0 \\ 0 & 0 & 0 & 0 \\ 0 & 0 & -L & -L^2 \end{bmatrix}_{8 \times 4},$$

and I_4 is the 4×4 identity matrix.

For linear orthotropic shells of revolution the relations between the stress resultants, σ, and the strains and changes of curvature, ϵ, of the middle surface are

$$\sigma = \mathbf{E}\,\epsilon \equiv$$

$$\equiv \begin{Bmatrix} n_\xi \\ n_\varphi \\ n_{\xi\varphi} \\ m_\xi \\ m_\varphi \\ m_{\xi\varphi} \end{Bmatrix} = \begin{bmatrix} B_{11} & B_{12} & & & & \\ B_{12} & B_{22} & & & & \\ & & B_{33} & & & \\ & & & D_{11} & D_{12} & \\ & & & D_{12} & D_{22} & \\ & & & & & D_{33} \end{bmatrix} \begin{Bmatrix} \epsilon_\xi \\ \epsilon_\varphi \\ \gamma_{\xi\varphi} \\ \kappa_\xi \\ \kappa_\varphi \\ \kappa_{\xi\varphi} \end{Bmatrix} \qquad (4\text{-}10)$$

in which

$$B_{11} = \frac{E_\xi h}{1 - \nu_\xi \nu_\varphi} \quad , \quad B_{22} = \frac{E_\varphi h}{1 - \nu_\xi \nu_\varphi} \quad ,$$

$$B_{12} = \frac{E_\xi h \nu_\varphi}{1 - \nu_\xi \nu_\varphi} = \frac{E_\varphi h \nu_\xi}{1 - \nu_\xi \nu_\varphi} \quad , \quad B_{33} = G_{\xi\varphi} h$$

and

$$D_{ij} = \frac{h^2}{12} B_{ij} \, . \tag{4-11}$$

The constants appearing in Equations (4-10) and (4-11) are defined as follows:

E_ξ , E_φ = Young's modulus of elasticity in the ξ and φ directions, respectively,

ν_ξ , ν_φ = Poisson's ratio corresponding to the ξ and φ directions, respectively,

$G_{\xi\varphi}$ = shearing modulus, and

h = thickness of the shell wall.

The strain displacement relations for a shell of revolution are given in Equation (A-6). The strains can be expressed in terms of the m-th displacement coefficients as

$$\epsilon^m = \mathbf{W}_m(\xi)\, \alpha^m \equiv$$

$$
\equiv \begin{Bmatrix} \epsilon^m \\ \epsilon^m_\varphi \\ \gamma^m_{\xi\varphi} \\ \kappa^m_\xi \\ \kappa^m_\varphi \\ \kappa^m_{\xi\varphi} \end{Bmatrix} = \begin{bmatrix}
K_\xi \xi & K_\xi \xi^2 & K_\xi \xi^3 & K_\xi \xi^4 & 0 & H_1 & 0 & 0 & 2H_1\xi & 3H_1\xi^2 & 0 & 0 \\
K_\varphi & K_\varphi \xi & K_\varphi \xi^3 & K_\varphi \xi^4 & H_2 & H_2\xi & H_3 & H_3\xi & H_2\xi^2 & H_2\xi^3 & H_3\xi^2 & H_3\xi^3 \\
0 & 0 & 0 & 0 & -H_3 & -H_3\xi & -H_2 & -H_2\xi+H_1 & -H_3\xi^2 & -H_3\xi^3 & -H_2\xi^2+2H_1\xi & -H_2\xi^3+3H_1\xi^2 \\
0 & H_7 & 2H_7\xi-2H_4 & 3H_7\xi^2-6H_4\xi & 0 & 0 & 0 & 0 & 0 & 0 & 0 & 0 \\
H_6 & H_6\xi-H_5 & H_6\xi^2-2H_5\xi & H_6\xi^3-3H_5\xi^2 & 0 & 0 & 0 & 0 & 0 & 0 & 0 & 0 \\
-H_9 & -H_9\xi+H_8 & -H_9\xi^2+2H_8\xi & -H_9\xi^3+3H_8\xi^2 & 0 & 0 & 0 & 0 & 0 & 0 & 0 & 0
\end{bmatrix}_{6\times 12} \begin{Bmatrix} \alpha^m_1 \\ \alpha^m_2 \\ \alpha^m_3 \\ \alpha^m_4 \\ \alpha^m_5 \\ \alpha^m_6 \\ \alpha^m_7 \\ \alpha^m_8 \\ \alpha^m_9 \\ \alpha^m_{10} \\ \alpha^m_{11} \\ \alpha^m_{12} \end{Bmatrix},
$$

(Equation (4-12))

in which

$$H_1 = \frac{1}{A}\ , \qquad H_4 = \frac{1}{A^2}\ ,$$

$$H_2 = \frac{R'}{AR}\ , \qquad H_5 = \frac{R'}{A^2R}\ ,$$

$$H_3 = \frac{m}{R}\ , \qquad H_6 = \frac{m^2}{R^2}\ ,$$

$$H_7 = \frac{R'R''}{A^4}\ ,$$

$$H_8 = \frac{2m}{AR}\ ,$$

$$H_9 = \frac{2mR'}{AR^2}\ ,$$

$$K_\xi = \frac{1}{R_\xi}\ , \quad \text{and} \quad K_\varphi = \frac{1}{R_\varphi}\ . \tag{4-13}$$

The strain energy of the shell element in terms of the internal strains and stresses is

$$\mathbf{U} = \frac{1}{2} \int_{\text{surface}} \epsilon^* \sigma \, dS \tag{4-14}$$

For the m-th harmonic this becomes

$$\mathbf{U}_m = \frac{1}{2}\, \alpha^{m*}\, \mathbf{L}^m\, \alpha^m \tag{4-15}$$

in which

$$\mathbf{L}^m = \int_0^{2\pi} \int_0^L \mathbf{W}_m^*(\xi)\, \mathbf{E}\, \mathbf{W}_m(\xi)\, A\, R \left\langle \begin{matrix} \sin^2 m\varphi \\ \cos^2 m\varphi \end{matrix} \right\rangle d\varphi\, d\xi \ .$$

The notation

$$\left\langle \begin{matrix} \sin^2 m\varphi \\ \cos^2 m\varphi \end{matrix} \right\rangle$$

indicates that only the squares of sines and cosines occur when the m-th Fourier terms are substituted into Equation (4-14). The surface element is given by

$$dS = A\,R\,d\xi\,d\varphi$$

in Equation (4-15). Substituting Equation (4-9) into Equation (4-15) one obtains

$$\mathbf{U}_m = \frac{1}{2}\left[q_m \,\vdots\, \alpha_b^m\right] \mathbf{M}^* \, \mathbf{L}^m \, \mathbf{M} \left\{\begin{matrix} q_m \\ \hdashline \alpha_b^m \end{matrix}\right\} . \tag{4-16}$$

The work done by the (external) boundary forces acting through the boundary displacements is

$$\mathbf{V}_m = \int_0^{2\pi} q_m^* \begin{bmatrix} a\,I_4 & 0 \\ 0 & a'\,I_4 \end{bmatrix} f_m \left\langle \begin{matrix} \sin^2 m\varphi \\ \cos^2 m\varphi \end{matrix} \right\rangle d\varphi \tag{4-17}$$

The radii, a and a′, of the boundary circles are shown on Figure 4-1b.

The total potential energy of the element for the m-th harmonic is

$$\Pi_m = \mathbf{U}_m - \mathbf{V}_m . \tag{4-18}$$

Comparison of Equations (4-15), (4-16), and (4-17) shows that the integral

$$\int_0^{2\pi} \left\langle \begin{matrix} \sin^2 m\varphi \\ \cos^2 m\varphi \end{matrix} \right\rangle d\varphi$$

occurs in both, $\mathbb{U}_m$ and $\mathbb{V}_m$, so that it may be factored from Π_m.

The condition of minimum potential energy,

$$\frac{\partial \Pi_m}{\partial q_{im}} = 0 \qquad i = 1,(1),8$$

$$\frac{\partial \Pi_m}{\partial \alpha^m_{bj}} = 0 \qquad j = 1,(1),4 \qquad ,$$

where q_{im} and α^m_{bj} are the elements of q_m and α^m_b, respectively, yields

$$\mathbb{M}^* \mathbf{G}^m \mathbb{M} \begin{Bmatrix} q_m \\ \hline \alpha^m_b \end{Bmatrix} = \left[\begin{array}{ccc} a\, I_4 & 0 & 0 \\ 0 & a' I_4 & 0 \\ \hline 0 & 0 & I_4 \end{array}\right] \begin{Bmatrix} f_m \\ \hline 0 \end{Bmatrix} \qquad (4\text{-}19)$$

in which

$$\mathbf{G}^m = \int_0^L \mathbb{W}^*_m(\xi)\ \mathbb{E}\ \mathbb{W}_m(\xi)\, A\, R\, dt \ .$$

Let

$$\mathbb{K}^m = \begin{bmatrix} \frac{1}{a} I_4 & 0 & 0 \\ 0 & \frac{1}{a'} I_4 & 0 \\ 0 & 0 & I_4 \end{bmatrix} \mathbb{M}^* \mathbf{G}^m \mathbb{M}' \equiv \left[\begin{array}{c|c} \underset{8\times 8}{\mathbb{K}^m_{aa}} & \underset{8\times 4}{\mathbb{K}^m_{ab}} \\ \hline \underset{4\times 8}{\mathbb{K}^m_{ba}} & \underset{4\times 4}{\mathbb{K}^m_{bb}} \end{array}\right] \ . \qquad (4\text{-}20)$$

With Equation (4-20) it is possible to eliminate α^m_b from Equation (4-19), so that

$$\left[\mathbb{K}^m_{aa} - \mathbb{K}^m_{ab} \left(\mathbb{K}^m_{bb} \right)^{-1} \mathbb{K}^m_{ba} \right] q_m = f_m \tag{4-21}$$

from which the desired stiffness matrix is obtained as

$$K_m = \mathbb{K}^m_{aa} - \mathbb{K}^m_{ab} \left(\mathbb{K}^m_{bb} \right)^{-1} \mathbb{K}^m_{ba} \ . \tag{4-22}$$

The computations involved in obtaining $\mathbf{G}_m$ are made on the computer by use of Weddle's seven point integration formula

$$\int_{x_o}^{x_o+6h} f(x) = \frac{3h}{10} \left(f_o + 5f_1 + f_2 + 6f_3 + f_4 + 5f_5 + f_6 \right) \ ,$$

where $$f_i \equiv f(x_o + ih) \qquad i = 0, (1), 6 \ . \tag{4-23}$$

For a cylindrical element the integration can be done analytically by letting $A(\xi) = 1$, and $R(\xi) = a' = a$. Equation (4-19) then becomes

$$\mathbf{G}^m = a \, \overline{\mathbf{G}}^m, \quad \text{where} \quad \overline{\mathbf{G}}^m = \int_0^L \mathbb{W}^*_m(\xi) \ \mathbf{E} \ \mathbb{W}_m(\xi) \, d\xi \tag{4-24}$$

and

$$\mathbb{M}^* \ \overline{\mathbf{G}}^m \ \mathbb{M} \begin{Bmatrix} q_m \\ \alpha_b \end{Bmatrix} = \begin{Bmatrix} f_m \\ 0 \end{Bmatrix} \ .$$

The individual terms of $\overline{\mathbf{G}}^m$ are listed in Section A.2 for comparison with the numerical integration using Weddle's formula.

4.3 FIXED EDGE FORCES

Fixed edge forces resulting from given loading functions are obtained by use of the principle of virtual work*. A necessary and sufficient condition for equilibrium of any linear structural system is that the virtual work for all virtual displacements is identically equal to zero. The virtual work of a force is its scalar product with the virtual displacements of its point of application.

Since the repetitive technique discussed in Section 2 requires proportionality between loading functions and deformation patterns, distributed loadings assume the following form

$$p_u(\xi,\varphi) = \sum_{m=0}^{\infty} p_u^m(\xi)\cos m\varphi$$

$$p_v(\xi,\varphi) = \sum_{m=0}^{\infty} p_v^m(\xi)\sin m\varphi \quad , \quad \text{and}$$

$$p_w(\xi,\varphi) = \sum_{m=0}^{\infty} p_w^m(\xi)\cos m\varphi \quad , \tag{4-25}$$

where

$$p_u^m(\xi) = \beta_5^m + \beta_6^m\xi + \beta_9^m\xi^2 + \beta_{10}^m\xi^3$$

$$p_v^m(\xi) = \beta_7^m + \beta_8^m\xi + \beta_{11}^m\xi^2 + \beta_{12}^m\xi^3 \quad , \text{ and}$$

$$p_w^m(\xi) = \beta_1^m + \beta_2^m\xi + \beta_3^m\xi^2 + \beta_4^m\xi^3 \quad . \tag{4-26}$$

---

*Johann Bernoulli, "Das Prinzip der virtuellen Verrückungen," Basle, Switzerland, January 26, 1717.

The coefficients β_i^m are labeled identically to the coefficients α_i^m in Equation (4-3), so that Equations (4-26) and (4-3) can be written as

$$\bar{p}^m(\xi) = \mathbb{F}(\xi)\,\beta^m \quad , \quad \text{and}$$

$$\bar{u}^m(\xi) = \mathbb{F}(\xi)\,\alpha^m \quad , \tag{4-27}$$

respectively, in which

$$\mathbb{F}(\xi) = \begin{pmatrix} 0 & 0 & 0 & 0 & 1 & \xi & 0 & 0 & \xi^2 & \xi^3 & 0 & 0 \\ 0 & 0 & 0 & 0 & 0 & 0 & 1 & \xi & 0 & 0 & \xi^2 & \xi^3 \\ 1 & \xi & \xi^2 & \xi^3 & 0 & 0 & 0 & 0 & 0 & 0 & 0 & 0 \end{pmatrix}_{3 \times 12}$$

$$\beta^m = \begin{Bmatrix} \beta_1^m \\ \beta_2^m \\ \beta_3^m \\ \cdot \\ \cdot \\ \cdot \\ \beta_{12}^m \end{Bmatrix} \quad , \quad \text{and} \quad \alpha^m = \begin{Bmatrix} \alpha_1^m \\ \alpha_2^m \\ \alpha_3^m \\ \cdot \\ \cdot \\ \cdot \\ \alpha_{12}^m \end{Bmatrix} \quad .$$

The coefficients α_i^m for any given boundary displacements are defined from Equations (4-8), (4-19), and (4-20) as

$$\alpha^m = \mathbb{D}^m\, q_m$$

where

$$\mathbb{D}^m = \begin{pmatrix} \mathbb{B}_a^{-1} + \mathbb{B}_a^{-1} \mathbb{B}_b \left(\mathbb{K}_{bb}^m\right)^{-1} \mathbb{K}_{ba}^m \\ \hdashline -\left(\mathbb{K}_{bb}^m\right)^{-1} \mathbb{K}_{ba}^m \end{pmatrix}_{12 \times 8} \tag{4-28}$$

therefore, from Equation (4-27)

$$\bar{u}^m(\xi) = \mathbb{F}(\xi)\ \mathbb{D}^m\ q_m \ . \tag{4-29}$$

The fixed edge forces as indicated on Figure 4-3 are represented in vector form as

$$f_m^f = \begin{Bmatrix} N_m^f \\ T_m^f \\ S_m^f \\ M_m^f \\ N_m^{f'} \\ T_m^{f'} \\ S_m^{f'} \\ M_m^{f'} \end{Bmatrix} .$$

For example, the derivation of one fixed edge quantity, the moment M_m^f, due to a loading $\bar{p}^m(\xi)$ is developed in detail below. As illustrated on Figure 4-4 a virtual rotation θ_{Mf}^m is applied at the left boundary of the element with all other boundary displacements restrained. The corresponding virtual displacement field is

$$\bar{u}^{m}_{Mf}(\xi) = \mathbf{F}(\xi)\ \mathbf{D}^{m} \begin{Bmatrix} 0 \\ 0 \\ 0 \\ \theta^{m}_{Mf} \\ 0 \\ 0 \\ 0 \\ 0 \end{Bmatrix} \tag{4-30}$$

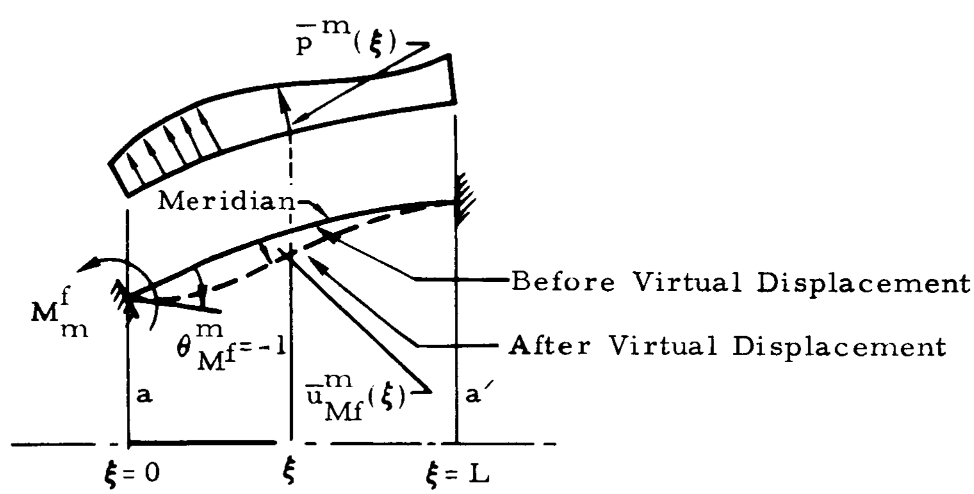

Figure 4-4 - Virtual Displacements on Element

The sum of all virtual work is

$$\int_0^{2\pi} M_m^f \, \theta_{Mf}^m \cos^2\varphi \; a \; d\varphi \; +$$

$$+ \int_0^{2\pi} \int_0^L \bar{u}_{Mf}^{m\,*}(\xi)\, \bar{p}^m(\xi)\, A\, R \left\langle \begin{matrix} \sin^2\varphi \\ \cos^2\varphi \end{matrix} \right\rangle d\varphi \, d\xi \;\equiv\; 0 \qquad (4\text{-}31)$$

As in the derivation of the stiffness matrix, the integrals

$$\int_0^{2\pi} \left\langle \begin{matrix} \sin^2\varphi \\ \cos^2\varphi \end{matrix} \right\rangle d\varphi$$

cancel out, so that, with

$$\theta_{Mf}^m = -1 \; ,$$

$$a \; M_m^f(-1) + \int_0^L \bar{u}_{Mf}^{m\,*}(\xi)\, \bar{p}^m(\xi)\, A\, R\, d\xi \;=\; 0 \qquad (4\text{-}32)$$

or

$$M_m^f = \frac{1}{a} \int_0^L \bar{u}_{Mf}^{m\,*}(\xi)\, \bar{p}^m(\xi)\, A\, R\, d\xi \; . \qquad (4\text{-}33)$$

The other fixed edge forces can be obtained in a similar manner. Using Equations (4-27), (4-28) and (4-29) and successively applying the above procedure for each fixed edge force, yields all the virtual work equations as

$$\begin{bmatrix} -a\, I_4 & 0 \\ \hline 0 & -a'\, I_4 \end{bmatrix} f_m^f$$

$$- \mathbf{D}^{m*} \left(\int_0^L \mathbf{F}^*(\xi)\, \mathbf{F}(\xi)\, A(\xi)\, R(\xi)\, d\xi \right) \beta^m \equiv 0 \tag{4-34}$$

Thus, the vector of fixed edge forces is given by

$$f_m^f = \begin{bmatrix} -\frac{1}{a}\, I_4 & 0 \\ \hline 0 & -\frac{1}{a'}\, I_4 \end{bmatrix} \mathbf{D}^{m*}\, \mathbf{S}\, \beta^m$$

where

$$\mathbf{S} = \int_0^L \mathbf{F}^*(\xi)\, \mathbf{F}(\xi)\, A(\xi)\, R(\xi)\, d\xi \tag{4-35}$$

For a cylindrical shell, $A = 1$, $R = a' = a$, and Equation (4-35) reduces to

$$f_m^f = - \mathbf{D}^{m*}\, \overline{\mathbf{S}}\, \beta^m$$

where

$$\overline{\mathbf{S}} = \int_0^L \mathbf{F}^*(\xi)\, \mathbf{F}(\xi)\, d\xi ,$$

which is

$$
\bar{S} = \left[\begin{array}{cccc:cccc:cccc}
L & \frac{L^2}{2} & \frac{L^3}{3} & \frac{L^4}{4} & & & & & & & & \\
\frac{L^2}{2} & \frac{L^3}{3} & \frac{L^4}{4} & \frac{L^5}{5} & & \Phi_4 & & & & \Phi_4 & & \\
\frac{L^3}{3} & \frac{L^4}{4} & \frac{L^5}{5} & \frac{L^6}{6} & & & & & & & & \\
\frac{L^4}{4} & \frac{L^5}{5} & \frac{L^6}{6} & \frac{L^7}{7} & & & & & & & & \\
\hdashline
 & & & & L & \frac{L^2}{2} & 0 & 0 & \frac{L^3}{3} & \frac{L^4}{4} & 0 & 0 \\
 & \Phi_4 & & & \frac{L^2}{2} & \frac{L^3}{3} & 0 & 0 & \frac{L^4}{4} & \frac{L^5}{5} & 0 & 0 \\
 & & & & 0 & 0 & L & \frac{L^2}{2} & 0 & 0 & \frac{L^3}{3} & \frac{L^4}{4} \\
 & & & & 0 & 0 & \frac{L^2}{2} & \frac{L^3}{3} & 0 & 0 & \frac{L^4}{4} & \frac{L^5}{5} \\
\hdashline
 & & & & \frac{L^3}{3} & \frac{L^4}{4} & 0 & 0 & \frac{L^5}{5} & \frac{L^6}{6} & 0 & 0 \\
 & \Phi_4 & & & \frac{L^4}{4} & \frac{L^5}{5} & 0 & 0 & \frac{L^6}{6} & \frac{L^7}{7} & 0 & 0 \\
 & & & & 0 & 0 & \frac{L^3}{3} & \frac{L^4}{4} & 0 & 0 & \frac{L^5}{5} & \frac{L^6}{6} \\
 & & & & 0 & 0 & \frac{L^4}{4} & \frac{L^5}{5} & 0 & 0 & \frac{L^6}{6} & \frac{L^7}{7}
\end{array}\right]_{12 \times 12} \tag{4-36}
$$

Section 5
NUMERICAL FORMULATION

A computer program, coded entirely in Fortran IV, was written to implement the formulation presented in Sections 2, 3, and 4. A flow chart is given on Figure 5-1.

Required input to the program are a minimum description of the geometrical and elastic properties of the whole shell, boundary conditions, harmonic number, and static loading functions from which the first approximation is computed for each mode shape.

The subroutine used to solve the eigenproblem

$$(\omega^2 M - K)\,\bar{c} = 0$$

is the one used by Whetstone and Pearson (1966). Only a few seconds of computer time are required by this routine to solve low ordered equations.

Two numerical errors are possible in static analysis of a shell by the state vector walk-through method:

1. Elements are too large for their behavior to be accurately described by cubic parabola displacement functions;
2. The number of elements is too large for successive transfer matrix multiplication to remain accurate.

Both of these errors were studied with a closely related but algebraically simpler problem of a rectangular plate with two opposite edges simply supported, thus enabling a single Fourier series solution as in the shell analysis. For comparison, the exact plate strip stiffness matrix and fixed edge forces are available from classical plate theory, Dean (1967).

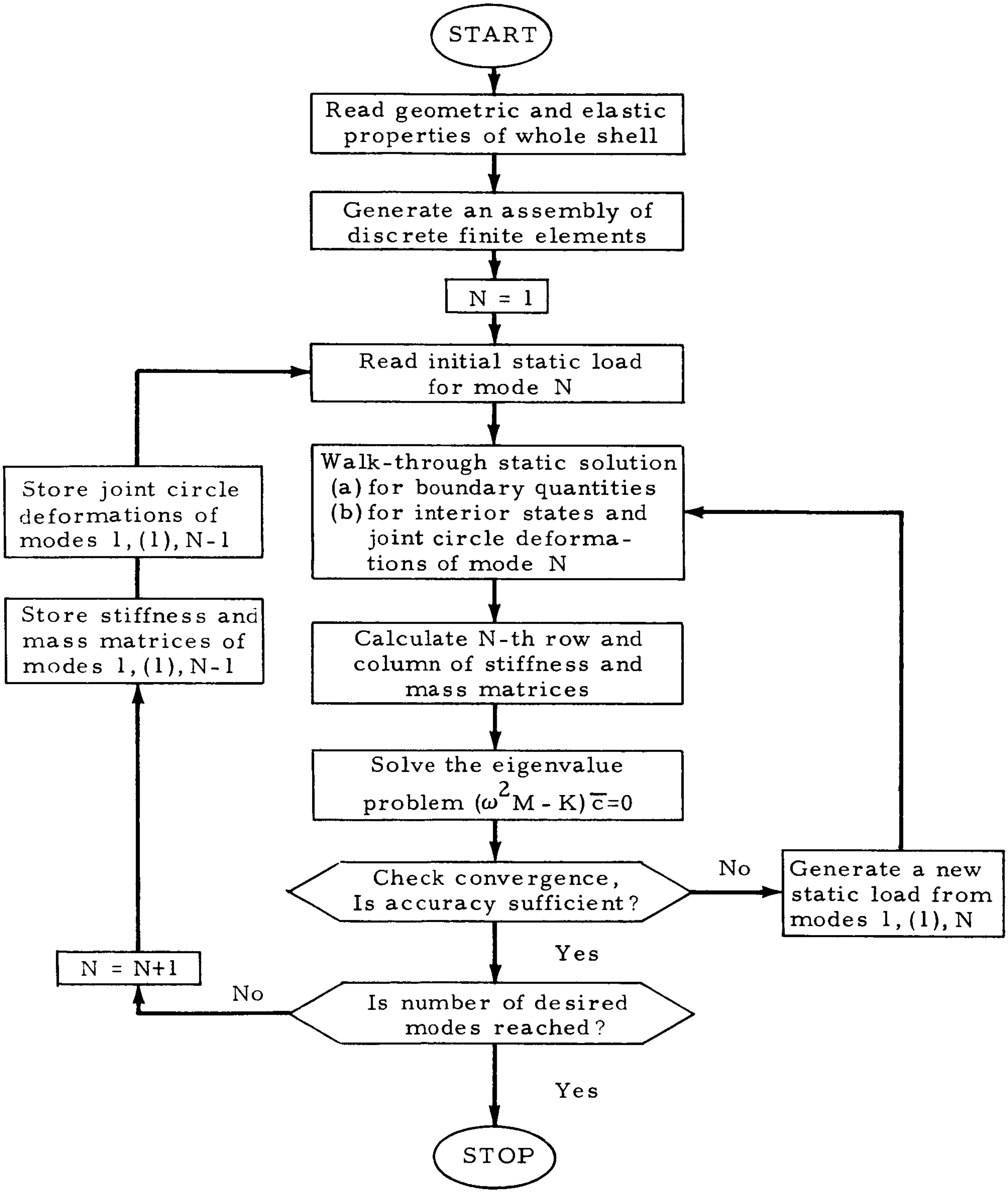

Figure 5-1 - Flow Chart of Computer Program

According to this reference, an asymptotic solution with a one-term correction was possible for a plate strip that complies with the condition

$$\left(\frac{m\pi a}{2b}\right)^2 << 1$$

where m = harmonic number, and a/b = aspect ratio of the strip (a is the width, b the length of the strip). This criterion was also found to be valid for an element with a cubic parabola displacement assumption.

In the case of a shell of revolution, a criterion to estimate element size is the wave length at which an edge disturbance penetrates into the shell. Approximately one-eighth of this wave length is the maximum element size to give a sufficiently accurate transfer matrix. For the zeroth harmonic, the "breathing"-mode, of a shell of revolution the wave length is approximately

$$L = \frac{2\pi}{\kappa} R_\varphi$$

where

$$\kappa^4 = 3(1 - \nu^2)\left(\frac{R_\varphi}{h}\right)^2$$

R_φ = principal radius of φ coordinate, and

h = thickness of the shell.

For higher harmonics this wave length becomes shorter; therefore, the corresponding element size should be reduced accordingly to retain the relative accuracy. For flexibility in the application, the program permits variable element sizes. Small elements may be used in regions of bending, and larger ones in regions where membrane action prevails.

Section 6
EXAMPLE PROBLEMS

6.1 RECTANGULAR PLATE

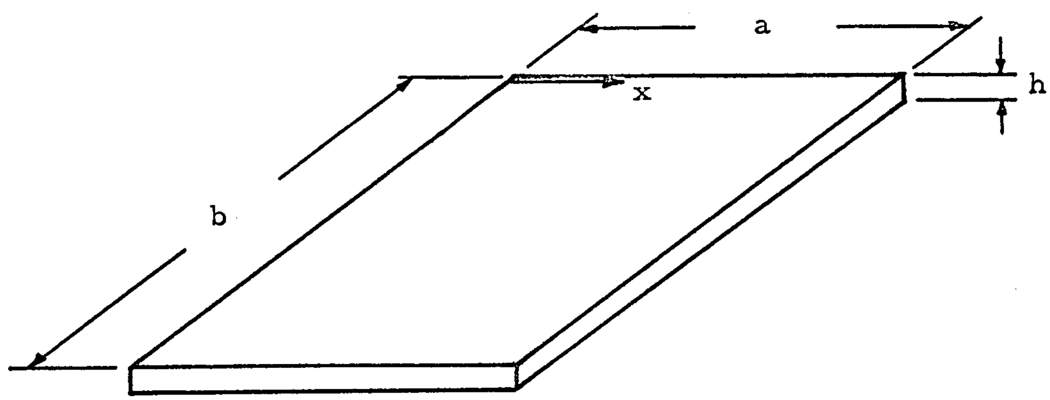

$a = b = 100$ in., $h = .714$ in., $E = 3 \times 10^7$ lbs/in^2,

$\nu = .3$, $\rho = 7.33 \times 10^{-4}$ lbs-sec^2/in^4,

Simple Side Support

Figure 6.1 - Rectangular Plate

The following frequencies were obtained for the first harmonic using 10 elements.

m = 1	1st Mode	2nd Mode
1st approximation	13.7621 cps	34.3716 cps
2nd approximation	13.7311 cps	34.3367 cps
3rd approximation	13.7311 cps	34.3367 cps
.	.	.
.	.	.
.	.	.
10th approximation	13.7311 cps	34.3367 cps

From classical plate theory, the frequencies are

$$f = \frac{\omega}{2\pi}, \quad \text{where} \quad \omega^2 = \frac{D}{\rho h}\left(\frac{i\pi^2}{a^2} + \frac{j\pi^2}{b^2}\right)^2$$

and

$$D = \frac{Eh^2}{12(1-\nu^2)}$$

For $i = j = 1$ this formula gives

$$f_{1,1} = 13.7309 \text{ cps} \qquad f_{1,2} = 34.3274 \text{ cps} .$$

The frequencies obtained for higher harmonics are as follows:

		1st Mode	2nd Mode
m = 2,	10th approximation	34.3275 cps	54.9418 cps
	classical theory	34.3274 cps	54.9438 cps
m = 3,	10th approximation	68.6545 cps	89.2527 cps
	classical theory	68.6548 cps	89.2512 cps .

Static solutions for sine-wave loadings were computed. The results for m = 1 and m = 5 are summarized below.

		$\frac{x}{a}$ =	.0	.1	.2	.3	.4	.5
<u>m = 1</u>								
computed displacements*	$w\left(\frac{x}{a}\right)$	=	.000	.07930	.15085	.20762	.24408	.25664
classical theory*	$w\left(\frac{x}{a}\right)$	=	.000	.07927	.15078	.20756	.24403	.25665
<u>m = 5</u>								
computed displacements**	$w\left(\frac{x}{a}\right)$	=	.000	.31074	.59016	.81073	.95160	1.0000
classical theory**	$w\left(\frac{x}{a}\right)$	=	.000	.309	.588	.809	.945	1.00

The computed displacements for m = 5 result from the 10th iteration on the first mode, using 100 elements.

*Normalized to a central deflection of $\dfrac{1.0}{D\left(\dfrac{\pi^2}{a^2} + \dfrac{\pi^2}{b^2}\right)^2}$

**Normalized to a central deflection of 1.0

6.2 CYLINDRICAL SHELL

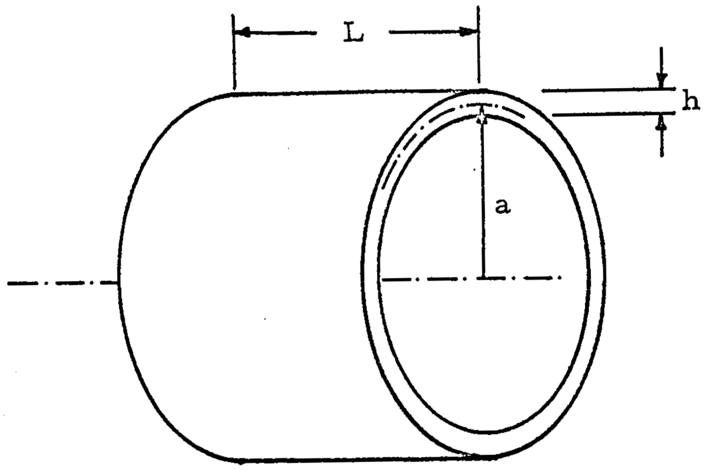

$a = 5$ in., $L = 1$ in., 2 in., 2.5 in., $h = .01$ in.
$E = 3 \times 10^7$ lbs/in^2, $\nu = .3$, $\rho = 7.33 \times 10^{-4}$ lbs-sec^2/in^4, boundary conditions:
left $U = V = W = M = 0$, right $N = V = W = M = 0$

Figure 6.2 - Cylindrical Shell

For $L = 1$ in., and $m = 0$, the sequence of frequency approximations computed by the program was:

	1st Mode	2nd Mode
1st approximation	6563.28 cps	7478.36 cps
2nd approximation	6483.48 cps	7459.97 cps
3rd approximation	6473.94 cps	7459.94 cps
4th approximation	6472.68 cps	7459.94 cps
5th approximation	6472.51 cps	7459.94 cps

Ten elements were used in the above solution. For comparison, the frequencies of a cylinder with $N = V = W = M = 0$ at the left and the right boundaries are computed from Donnell's equation:

$$f = \frac{\omega}{2\pi}, \quad \text{where} \quad \omega^2 = \frac{\bar{\lambda}^2 E}{(1-\nu^2)a^2},$$

$$\bar{\lambda}^2 = 1 + c^2 \alpha_j^4,$$

$$c^2 = \frac{h^2}{12a^2(1-\nu^2)}, \quad \text{and} \quad \alpha_j = \frac{j\pi a}{L}.$$

For $j = 1, 2$

$$f_1 = 6820 \text{ cps}, \quad f_2 = 7810 \text{ cps}.$$

These results are slightly higher because Donnell's equations do not account for in-plane inertia.

For $L = 2$ in., and $m = 0$, the frequency approximations are, with 20 elements

	1st Mode	2nd Mode
1st approximation	6467.34 cps	6569.46 cps
2nd approximation	6426.56 cps	6594.61 cps
3rd approximation	6415.87 cps	6564.17 cps
4th approximation	6410.59 cps	6583.99 cps
5th approximation	6407.21 cps	6566.82 cps

and with 10 elements

	1st Mode	2nd Mode
1st approximation	6466.37 cps	6567.86 cps
2nd approximation	6426.67 cps	6593.80 cps
3rd approximation	6415.99 cps	6563.61 cps
4th approximation	6410.71 cps	6584.10 cps
5th approximation	6407.31 cps	6565.00 cps

For $L = 2.5$ in., $m = 0$, and 25 elements the computed frequencies are

	1st Mode	2nd Mode
1st approximation	6443.05 cps	6618.34 cps
2nd approximation	6409.48 cps	6459.09 cps
3rd approximation	6400.73 cps	6679.87 cps
4th approximation	6396.12 cps	6470.69 cps
5th approximation	6393.89 cps	6670.64 cps

The results indicate that a few more iterations would be required for complete convergence.

Static solutions corresponding to a uniform rotationally symmetric pressure loading are summarized in Table 6-1.

Table 6-1

Static Solutions, Cylindrical Shell (m=0)

℄

L = 1 in

	Radial Deflections (in.) x 10^{-4}						Bending Moments (in-lbs/in.) x 10^{-2}					
10 Elements	.00000	.43916	.72712	.86570	.91408	.92385	.04466	.09812	.24486	.42149	.45539	.00000
Classical Theory	.00000	.43911	.72706	.86568	.91409	.92388	.04474	.09818	.24486	.42139	.45523	.00000

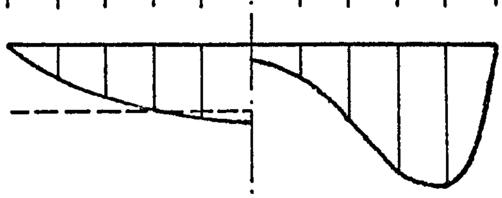

L = 2 in.

	Radial Deflections (in.) x 10^{-4}						Bending Moments (in-lbs/in.) x 10^{-2}					
10 Elements	(.00000)	(.72671)	(.88922)	(.85834)	(.83349)	(.82877)	(-.00474)	(-.01417)	(-.01446)	(.11264)	(.43900)	(.00000)
20 Elements	.00000	.72552	.88908	.85860	.83359	.82876	-.00489	-.01424	-.01410	.11324	.43742	.00000
Classical Theory	.00000	.72546	.88907	.85862	.83359	.82876	-.00491	-.01424	-.01407	.11328	.43733	.00000

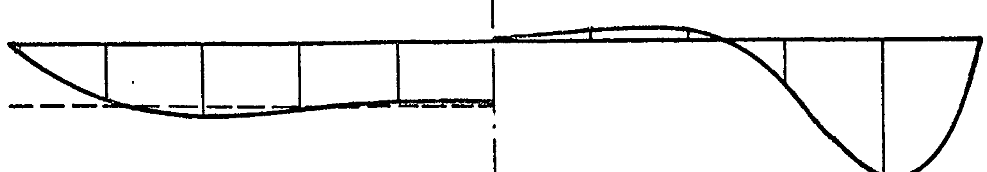

Table 6-1 (continued)

Radial Deflections (in.)

	x 10^{-4}												
25 Elements	.00000	.43978	.72550	.85611	.88899	.87869	.85855	.84280	.83432	.83131	.83115	.83188	.83245
Classical Theory	.00000	.43972	.72544	.85608	.88899	.87870	.85857	.84281	.83432	.83131	.83115	.83189	.83247

Bending Moments (in-lbs/in.)

													x 10^{-2}
25 Elements	.00168	.00060	-.00224	-.00762	-.01515	-.02093	-.01460	.02251	.11320	.26652	.43746	.46315	.00000
Classical Theory	.00167	.00058	-.00226	-.00763	-.01515	-.02093	-.01457	.02252	.11324	.26652	.43737	.46299	.00000

℄

L = 2.5 in.

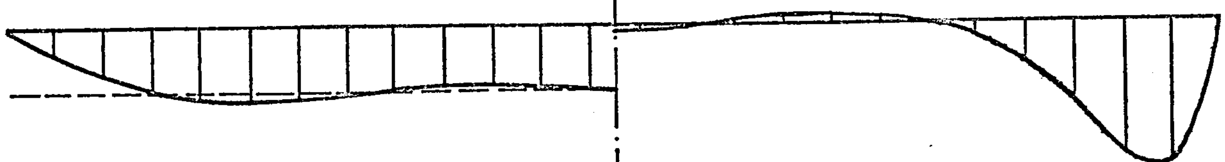

Section 7
REFERENCES

1. Cohen, G.A., "Computer Analysis of Asymmetric Deformation of Orthotropic Shells of Revolution," AIAA J. 2(5), pp. 932 - 934, May 1964.

2. Cohen, G.A., "Computer Analysis of Asymmetric Free Vibrations of Orthotropic Shells of Revolution," AIAA Paper No. 65-109, January 1965.

3. Cohen, G.A., "Computer Analysis of Asymmetric Free Vibrations of Ring-Stiffened Orthotropic Shells of Revolution," AIAA J. 3(12), pp. 2305 - 2312, December 1965.

4. Gallagher, R.H., "Techniques for the Derivation of Element Stiffness Matrices," AIAA J. 1(6), pp. 1431 - 1432, June 1963.

5. Greenbaum, G.A., Comments on "Numerical Analysis of Unsymmetrical Bending of Shells of Revolution," by Budiansky and Radkowski, AIAA J. 2(3), pp. 590 - 591, March 1964.

6. Kalnins, A., "Free Vibration of Rotationally Symmetric Shells," J. Acoust. Soc. Amer. 36(7), pp. 1355 - 1365, July 1964.

7. Kalnins, A., "Analysis of Shells of Revolution Subjected to Symmetrical and Nonsymmetrical Loads," J. Appl. Mech., Trans. ASME, pp. 467 - 476, September 1964.

8. Kalnins, A., "Dynamic Problems of Elastic Shells," Appl. Mech. Reviews, 13(11), pp. 867 - 872, November 1965.

9. Kalnins, A., "On Free and Forced Vibration of Rotationally Symmetric Layered Shells," J. Appl. Mech., Trans. ASME, pp. 941 - 943, December 1965.

10. Klein, S., "Matrix Analysis of Shell Structures," M.S. Thesis, MIT, Cambridge, Mass., June 1964.

11. McDonald, D., "Vibration Characteristics of Thin Shells of Revolution," TM 54/20-14, LMSC/HREC A710769, Lockheed Missiles & Space Company, 1965.

12. McDonald, D. and D.L. Dean, "Lectures on Shells and Folded Plate Structures," Dept. of Civil Engineering, N.C. State Univ., Raleigh, N.C., May 1967.

13. Pian, T.H.H., "Derivation of Element Stiffness Matrices," AIAA J., 2(3), pp. 576 - 577, March 1964.

14. Ross, E. R. Jr., Comment on "Computer Analysis of Asymmetric Free Vibrations of Ring-Stiffened Orthotropic Shells of Revolution," AIAA J. 4(7), pp. 1310 - 1312, July 1966.

15. Whetstone, W.D. and M.L. Pearson, "Vibrational Characteristics of Large Complex Space Vehicles," LMSC/HREC A783589, Lockheed Missiles & Space Company, Huntsville, Alabama, 1966.

16. Whetstone, W.D. and C.E. Jones, "Vibrational Characteristics of Linear Space Frames," LMSC/HREC A784826, Lockheed Missiles & Space Company, Huntsville, Alabama, 1968.

APPENDIX

APPENDIX

A.1 EQUATIONS OF LINEAR SHELL THEORY

The length of a line element on a shell surface in orthogonal coordinates is

$$d_s = \left(A_1^2\,dx_1^2 + A_2^2\,dx_2^2\right)^{1/2} \tag{A-1}$$

The strain displacement relations for the middle surface of a thin shallow shell are given by

$$\epsilon_1 = \frac{1}{A_1} u_{,1} + \frac{A_{1,2}}{A_1 A_2} v + \frac{1}{R_1} w \quad ,$$

$$\epsilon_2 = \frac{1}{A_2} v_{,2} + \frac{A_{2,1}}{A_1 A_2} u + \frac{1}{R_2} w \quad ,$$

$$\gamma_{12} = \frac{A_1}{A_2}\left(\frac{u}{A_1}\right)_{,2} + \frac{A_2}{A_1}\left(\frac{v}{A_2}\right)_{,1} \quad ,$$

$$\kappa_1 = -\frac{1}{A_1}\left(\frac{w_{,1}}{A_1}\right)_{,1} - \frac{A_{1,2}}{A_1 A_2^2} w_{,2} \quad ,$$

$$\kappa_2 = -\frac{1}{A_2}\left(\frac{w_{,2}}{A_1}\right)_{,2} - \frac{A_{2,1}}{A_1^2 A_2} w_{,1} \quad , \text{ and}$$

$$\kappa_{12} = \frac{2}{A_1 A_2}\left(\frac{A_{1,2}}{A_1} w_{,1} + \frac{A_{2,1}}{A_2} w_{,2} - w_{,12}\right), \tag{A-2}$$

where

$$(\ )_{,1} = \frac{\partial}{\partial x_1}(\ ) \qquad \text{and} \qquad (\ )_{,2} = \frac{\partial}{\partial x_2}(\ ) \ .$$

For a shell of revolution in cylindrical coordinates, the position vector of any point on the middle surface is given by

$$\vec{R}(t, \varphi) = R(\xi)\vec{1}_r + Z(\xi)\vec{1}_z \tag{A-3}$$

in which $\vec{1}_r$ and $\vec{1}_z$ are the unit vectors in the radial and axial directions, respectively. The coordinates, ξ and φ, correspond to x_1 and x_2, respectively, and represent the length along the axis of revolution and the angle of longitude, as illustrated on Figure A-1.

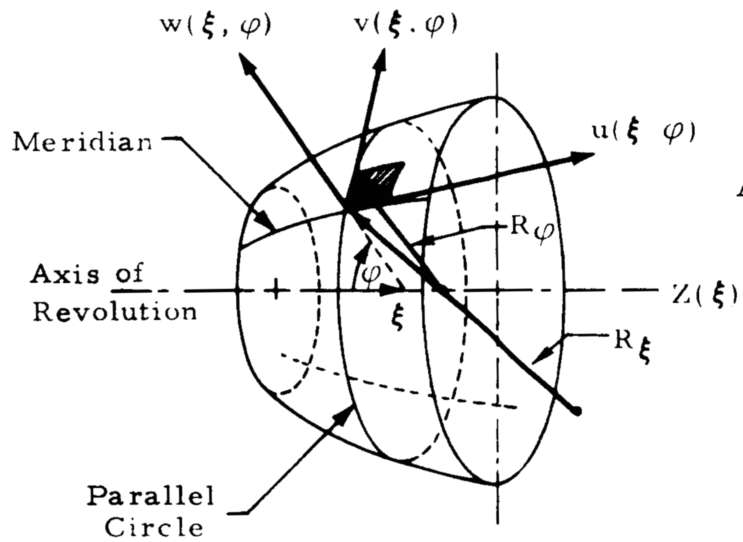

(a) Isometric View of Frustum

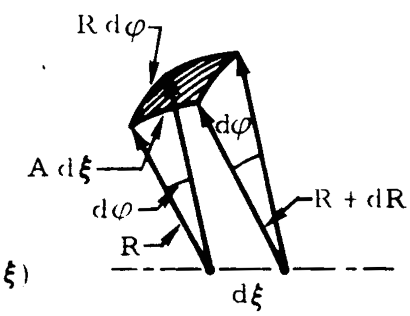

(b) Surface Element

Figure A-1 - Geometry of Shell of Revolution

For a cylindrical coordinate system, the metric coefficients of Equations (A-1) and (A-2) are

$$A_\xi = \sqrt{R'^2 + 1} = A , \quad \text{and} \quad A_\varphi = R , \tag{A-4}$$

and the principal curvatures are

$$K_\xi = \frac{1}{R_\xi} = -\frac{R''}{(R'^2 + 1)^{3/2}} = -\frac{R''}{A^3} , \text{ and}$$

$$K_\varphi = \frac{1}{R_\varphi} = \frac{1}{R(R'^2 + 1)^{1/2}} = \frac{1}{RA} . \tag{A-5}$$

The principal radii are shown on Figure A-1a and the metric coefficients on Figure A-1b.

Using these coefficients and curvatures in Equations (A-2), one obtains the strain displacement relations for a shell of revolution in cylindrical coordinates as

$$\epsilon_\xi = \frac{1}{A} u' + \frac{1}{R_\xi} w ,$$

$$\epsilon_\varphi = \frac{1}{R} \dot{v} + \frac{R'}{AR} u + \frac{1}{R_\varphi} w ,$$

$$\gamma_{\xi\varphi} = \frac{1}{R} \dot{u} + \frac{1}{A} v' - \frac{R'}{AR} v ,$$

$$\kappa_\xi = -\frac{1}{A^2} w'' + \frac{R'R''}{A^4} w' ,$$

$$\kappa_\varphi = -\frac{1}{R^2} \ddot{w} - \frac{R'}{A^2 R} w' , \text{ and}$$

$$\kappa_{\xi\varphi} = -\frac{2}{AR} \dot{w}' + \frac{2R'}{AR^2} \dot{w} , \tag{A-6}$$

where

$$(\ )' = \frac{\partial}{\partial \xi} \qquad \text{and} \qquad (\ )^{\cdot} = \frac{\partial}{\partial \varphi} .$$

A.2 INTEGRAL TERMS OF THE STIFFNESS MATRIX FOR A CYLINDRICAL ELEMENT

The integral for a cylindrical shell element as derived in Section 4 is given by

$$\overline{\mathbf{G}}^m = \int_o^L \mathbf{W}_m^*(\xi)\, \mathbf{E}\, \mathbf{W}_m(\xi)\, d\xi$$

The terms of $\overline{\mathbf{G}}_m$ are

$$\overline{G}_{11} = \left(B_{22}\frac{1}{a^2} + D_{22}\frac{m^4}{a^4}\right) L \ ,$$

$$\overline{G}_{12} = \left(B_{22}\frac{1}{a^2} + D_{22}\frac{m^4}{a^4}\right) \frac{L^2}{2} \ ,$$

$$\overline{G}_{13} = \left(B_{22}\frac{1}{a^2} + D_{22}\frac{m^4}{a^4}\right) \frac{L^3}{3} - 2D_{12}\frac{m^2}{a^2} L \ ,$$

$$\overline{G}_{14} = \left(B_{22}\frac{1}{a^2} + D_{22}\frac{m^4}{a^4}\right) \frac{L^4}{4} - 6D_{12}\frac{m^2}{a^2} \frac{L^2}{2} \ ,$$

$$\overline{G}_{15} = 0 \ ,$$

$$\overline{G}_{16} = B_{12}\frac{1}{a} L \ ,$$

$$\overline{G}_{17} = B_{22} \frac{m}{a^2} L \quad ,$$

$$\overline{G}_{18} = B_{22} \frac{m}{a^2} \frac{L^2}{2} \quad ,$$

$$\overline{G}_{19} = 2 B_{12} \frac{1}{a} \frac{L^2}{2} \quad ,$$

$$\overline{G}_{1,10} = 3 B_{12} \frac{1}{a} \frac{L^3}{3} \quad ,$$

$$\overline{G}_{1,11} = B_{22} \frac{m}{a^2} \frac{L^3}{3} \quad ,$$

$$\overline{G}_{1,12} = B_{22} \frac{m}{a^2} \frac{L^4}{4} \quad ,$$

$$\overline{G}_{22} = \left(B_{22} \frac{1}{a^2} + D_{22} \frac{m^4}{a^4} \right) \frac{L^3}{3} + 4 D_{33} \frac{m^2}{a^2} L \quad ,$$

$$\overline{G}_{23} = \left(B_{22} \frac{1}{a^2} + D_{22} \frac{m^4}{a^4} \right) \frac{L^4}{4} + \left(-2 D_{12} \frac{m^2}{a^2} + 8 D_{33} \frac{m^2}{a^2} \right) \frac{L^2}{2} \quad ,$$

$$\overline{G}_{24} = \left(B_{22} \frac{1}{a^2} + D_{22} \frac{m^4}{a^4} \right) \frac{L^5}{5} + \left(-6 D_{12} \frac{m^2}{a^2} + 12 D_{33} \frac{m^2}{a^2} \right) \frac{L^3}{3} \quad ,$$

$$\overline{G}_{25} = 0 \quad ,$$

$$\overline{G}_{26} = B_{12} \frac{1}{a} \frac{L^2}{2} \quad ,$$

$$\overline{G}_{27} = B_{22} \frac{m}{a^2} \frac{L^2}{2}$$

$$\overline{G}_{28} = B_{22} \frac{m}{a^2} \frac{L^3}{3}$$

$$\overline{G}_{29} = 2 B_{12} \frac{1}{a} \frac{L^3}{3}$$

$$\overline{G}_{2,10} = 3 B_{12} \frac{1}{a} \frac{L^4}{4}$$

$$\overline{G}_{2,11} = B_{22} \frac{m}{a^2} \frac{L^4}{4}$$

$$\overline{G}_{2,12} = B_{22} \frac{m}{a^2} \frac{L^5}{5}$$

$$\overline{G}_{33} = \left(B_{22} \frac{1}{a^2} + D_{22} \frac{m^4}{a^4}\right) \frac{L^5}{5} + \left(-4 D_{12} \frac{m^2}{a^2} + 16 D_{33} \frac{m^2}{a^2}\right) \frac{L^3}{3} + 4 D_{11} L \quad ,$$

$$\overline{G}_{34} = \left(B_{22} \frac{1}{a^2} + D_{22} \frac{m^4}{a^4}\right) \frac{L^6}{6} + \left(-8 D_{12} \frac{m^2}{a^2} + 24 D_{33} \frac{m^2}{a^2}\right) \frac{L^4}{4} + 12 D_{11} \frac{L^2}{2} \quad ,$$

$$\overline{G}_{35} = 0 \quad ,$$

$$\overline{G}_{36} = B_{12} \frac{1}{a} \frac{L^3}{3} \quad ,$$

$$\overline{G}_{37} = B_{22} \frac{m}{a^2} \frac{L^3}{3} \quad ,$$

$$\overline{G}_{38} = B_{22} \frac{m}{a^2} \frac{L^4}{4} \quad ,$$

$$\overline{G}_{39} = 2\,B_{12} \frac{1}{a} \frac{L^4}{4} \quad ,$$

$$\overline{G}_{3,10} = 3\,B_{12} \frac{1}{a} \frac{L^5}{5} \quad ,$$

$$\overline{G}_{3,11} = B_{22} \frac{m}{a^2} \frac{L^5}{5} \quad ,$$

$$\overline{G}_{3,12} = B_{22} \frac{m}{a^2} \frac{L^6}{6} \quad ,$$

$$\overline{G}_{44} = \left(B_{22} \frac{1}{a^2} + D_{22} \frac{m^4}{a^4}\right) \frac{L^7}{7} + \left(-12\,D_{12} \frac{m^2}{a^2} + 36\,D_{33} \frac{m^2}{a^2}\right) \frac{L^5}{5} + 36\,D_{11} \frac{L^3}{3} \quad ,$$

$$\overline{G}_{45} = 0 \quad ,$$

$$\overline{G}_{46} = B_{12} \frac{1}{a} \frac{L^4}{4} \quad ,$$

$$\overline{G}_{47} = B_{22} \frac{m}{a^2} \frac{L^4}{4} \quad ,$$

$$\overline{G}_{48} = B_{22} \frac{m}{a^2} \frac{L^5}{5} ,$$

$$\overline{G}_{49} = 2 B_{12} \frac{1}{a} \frac{L^5}{5} ,$$

$$\overline{G}_{4,10} = 3 B_{12} \frac{1}{a} \frac{L^6}{6} ,$$

$$\overline{G}_{4,11} = B_{22} \frac{m}{a^2} \frac{L^6}{6} ,$$

$$\overline{G}_{4,12} = B_{22} \frac{m}{a^2} \frac{L^7}{7} ,$$

$$\overline{G}_{55} = B_{33} \frac{m^2}{a^2} L ,$$

$$\overline{G}_{56} = B_{33} \frac{m^2}{a^2} \frac{L^2}{2} ,$$

$$\overline{G}_{57} = 0 ,$$

$$\overline{G}_{58} = - B_{33} \frac{m}{a} L ,$$

$$\overline{G}_{59} = - B_{33} \frac{m^2}{a^2} \frac{L^3}{3} ,$$

$$\overline{G}_{5,10} = - B_{33} \frac{m^2}{a^2} \frac{L^4}{4} ,$$

$$\overline{G}_{5,11} = -2B_{33}\frac{m}{a}\frac{L^2}{2} ,$$

$$\overline{G}_{5,12} = -3B_{33}\frac{m}{a}\frac{L^3}{3} ,$$

$$\overline{G}_{66} = B_{11}L + B_{33}\frac{m^2}{a^2}\frac{L^3}{3} ,$$

$$\overline{G}_{67} = B_{12}\frac{m}{a}L ,$$

$$\overline{G}_{68} = \left(B_{12}\frac{m}{a} - B_{33}\frac{m}{a}\right)\frac{L^2}{2} ,$$

$$\overline{G}_{69} = 2B_{11}\frac{L^2}{2} + B_{33}\frac{m^2}{a^2}\frac{L^4}{4} ,$$

$$\overline{G}_{6,10} = 3B_{11}\frac{L^3}{3} + B_{33}\frac{m^2}{a^2}\frac{L^5}{4} ,$$

$$\overline{G}_{6,11} = \left(B_{12}\frac{m}{a} - 2B_{33}\frac{m}{a}\right)\frac{L^3}{3} ,$$

$$\overline{G}_{6,12} = \left(B_{12}\frac{m}{a} - 3B_{33}\frac{m}{a}\right)\frac{L^4}{4} ,$$

$$\overline{G}_{77} = B_{22}\frac{m^2}{a^2}L ,$$

$$\overline{G}_{78} = B_{22}\frac{m^2}{a^2}\frac{L^2}{2} ,$$

$$\overline{G}_{79} = 2\,B_{12}\,\frac{m}{a}\,\frac{L^2}{2} \quad ,$$

$$\overline{G}_{7,10} = 3\,B_{12}\,\frac{m}{a}\,\frac{L^3}{3} \quad ,$$

$$\overline{G}_{7,11} = B_{22}\,\frac{m^2}{a^2}\,\frac{L^3}{3} \quad ,$$

$$\overline{G}_{7,12} = B_{22}\,\frac{m^2}{a^2}\,\frac{L^4}{4} \quad ,$$

$$\overline{G}_{88} = B_{22}\,\frac{m^2}{a^2}\,\frac{L^3}{3} + B_{33}\,L \quad ,$$

$$\overline{G}_{89} = \left(2\,B_{12}\,\frac{m}{a} - B_{33}\,\frac{m}{a}\right)\frac{L^3}{3} \quad ,$$

$$\overline{G}_{8,10} = \left(3\,B_{12}\,\frac{m}{a} - B_{33}\,\frac{m}{a}\right)\frac{L^4}{4} \quad ,$$

$$\overline{G}_{8,11} = B_{22}\,\frac{m^2}{a^2}\,\frac{L^4}{4} + 2\,B_{33}\,\frac{L^2}{2} \quad ,$$

$$\overline{G}_{8,12} = B_{22}\,\frac{m^2}{a^2}\,\frac{L^5}{5} + 3\,B_{33}\,\frac{L^3}{3} \quad ,$$

$$\overline{G}_{99} = 4\,B_{11}\,\frac{L^3}{3} + B_{33}\,\frac{m^2}{a^2}\,\frac{L^5}{5} \quad ,$$

$$\overline{G}_{9,10} = 6\,B_{11}\,\frac{L^4}{4} + B_{33}\,\frac{m^2}{a^2}\,\frac{L^6}{6} \quad ,$$

$$\overline{G}_{9,11} = \left(2 B_{12} \frac{m}{a} - 2 B_{33} \frac{m}{a}\right) \frac{L^4}{4} ,$$

$$\overline{G}_{9,12} = \left(2 B_{12} \frac{m}{a} - 3 B_{33} \frac{m}{a}\right) \frac{L^5}{5} ,$$

$$\overline{G}_{10,10} = 9 B_{11} \frac{L^5}{5} + B_{33} \frac{m^2}{a^2} \frac{L^7}{7} ,$$

$$\overline{G}_{10,11} = \left(3 B_{12} \frac{m}{a} - 2 B_{33} \frac{m}{a}\right) \frac{L^5}{5} ,$$

$$\overline{G}_{10,12} = \left(3 B_{12} \frac{m}{a} - 3 B_{33} \frac{m}{a}\right) \frac{L^6}{6} ,$$

$$\overline{G}_{11,11} = B_{22} \frac{m^2}{a^2} \frac{L^5}{5} + 4 B_{33} \frac{L^3}{3} ,$$

$$\overline{G}_{11,12} = B_{22} \frac{m^2}{a^2} \frac{L^6}{6} + 6 B_{33} \frac{L^4}{4} ,$$

$$\overline{G}_{12,12} = B_{22} \frac{m^2}{a^2} \frac{L^7}{7} + 9 B_{33} \frac{L^5}{5} , \quad \text{and}$$

$$\overline{G}_{ij} = \overline{G}_{ji} \qquad i, j = 1, (1), 12 . \tag{A-8}$$

A.3 PERMUTATION MATRICES FOR VARIOUS BOUNDARY CONDITIONS

The boundary state vectors, s, are partitioned into known and unknown quantities by use of permutation matrices, P_s, so that

$$\left\{ \begin{array}{c} \overline{s}_k \\ \hline \overline{s}_u \end{array} \right\} = \overline{s} = P_s \, s \tag{A-9}$$

as indicated in Equation (3-15). A permutation matrix contains the property of orthogonality, expressed as

$$P_s^{-1} = P_s^{*} \tag{A-10}$$

The following is a listing of the permutation matrices arising from various boundary conditions.

(a) freely supported

$$N = V = W = M = 0$$

$$\bar{s} \equiv \begin{bmatrix} 0 \\ 0 \\ 0 \\ 0 \\ U \\ T \\ S \\ \theta \end{bmatrix} = \begin{bmatrix} 0 & 0 & 0 & 0 & 1 & 0 & 0 & 0 \\ 0 & 1 & 0 & 0 & 0 & 0 & 0 & 0 \\ 0 & 0 & 1 & 0 & 0 & 0 & 0 & 0 \\ 0 & 0 & 0 & 0 & 0 & 0 & 0 & 1 \\ 1 & 0 & 0 & 0 & 0 & 0 & 0 & 0 \\ 0 & 0 & 0 & 0 & 0 & 1 & 0 & 0 \\ 0 & 0 & 0 & 0 & 0 & 0 & 1 & 0 \\ 0 & 0 & 0 & 1 & 0 & 0 & 0 & 0 \end{bmatrix} \begin{Bmatrix} U \\ V=0 \\ W=0 \\ \theta \\ N=0 \\ T \\ S \\ M=0 \end{Bmatrix} \equiv P_s\, s$$

(b) fixed

$$U = V = W = \theta = 0$$

$$P_s = I_8$$

(c) free

$$N = T = S = M = 0$$

$$P_s = \left[\begin{array}{c|c} \Phi_4 & I_4 \\ \hline I_4 & \Phi_4 \end{array}\right]$$

(d) guided-free

$$U = V = S = \theta = 0$$

$$P_s = \begin{bmatrix} 1 & 0 & 0 & 0 & 0 & 0 & 0 & 0 \\ 0 & 1 & 0 & 0 & 0 & 0 & 0 & 0 \\ 0 & 0 & 0 & 0 & 0 & 0 & 1 & 0 \\ 0 & 0 & 0 & 1 & 0 & 0 & 0 & 0 \\ 0 & 0 & 0 & 0 & 1 & 0 & 0 & 0 \\ 0 & 0 & 0 & 0 & 0 & 1 & 0 & 0 \\ 0 & 0 & 1 & 0 & 0 & 0 & 0 & 0 \\ 0 & 0 & 0 & 0 & 0 & 0 & 0 & 1 \end{bmatrix}$$

(e) pole

A shell pole requires special attention regarding the harmonic in question, according to Greenbaum (1964). There are three cases

$m = 0 \qquad U = V = S = \theta = 0$ (guided free)

$m = 1 \qquad U + V = T = W = M = 0$

$m = 2 \qquad U = V = W = \theta = 0$ (fixed)